



Twenty-six moment equations for the Enskog–Vlasov equation

Henning Struchtrup^{1,†} and Aldo Frezzotti²

¹University of Victoria, Victoria, BC V8W 2Y2, Canada

²Politecnico di Milano, 20133 Milano, Italy

(Received 31 August 2021; revised 15 December 2021; accepted 26 January 2022)

The Enskog–Vlasov equation is a phenomenological kinetic equation that extends the Enskog equation for the dense (non-ideal) hard-sphere fluid by adding an attractive soft potential tail to the purely repulsive hard-sphere contribution. Simplifying assumptions about pair correlations lead to a Vlasov-like self-consistent force field that adds to the Enskog non-local hard-sphere collision integral. Within the limitations imposed by the underlying assumptions, the extension gives the Enskog–Vlasov equation the ability to give a unified description of ideal and non-ideal fluid flows as well as of those fluid states in which liquid and vapour regions coexist, being separated by a resolved interface. Furthermore, the Enskog–Vlasov fluid can be arbitrarily far from equilibrium. Thus the Enskog–Vlasov model equation provides an excellent, although approximate, tool for modelling processes with liquid–vapour interfaces and adjacent Knudsen layers, and allows us to look at slip, jump and evaporation coefficients from a different perspective. Here, a set of 26 moment equations is derived from the Enskog–Vlasov equation by means of the Grad moment method. The equations provide a meaningful approximation to the underlying kinetic equation, and include the description of Knudsen layers. This work focuses on the – rather involved – derivation of the moment equations, with only a few applications shown.

Key words: condensation/evaporation, kinetic theory, microscale transport

1. Introduction

The work described in the present paper originates from the authors' interest in the theory of evaporation/condensation flows from the point of view of the kinetic theory of fluids. Therefore, it is perhaps in order to summarize some of the relevant aspects behind the motivation of the developments described below.

† Email address for correspondence: struchtr@uvic.ca

In hydrodynamic modelling of flows in which liquid and vapour regions coexist, the details of the liquid–vapour interface are often ignored, and the actual interface is replaced by a sharp boundary between the two phases. Modelling of transport processes across the interface then requires interface conditions that relate properties of the two adjacent phases to supplement conservation of mass, energy and momentum across the interface (Hertz 1882; Knudsen 1915; Schrage 1953; Kjelstrup & Bedeaux 2008).

In classical hydrodynamics, which is applicable to a large number of engineering problems, one typically assumes continuity of temperature and tangential velocity, so that there is neither a temperature jump nor a tangential slip velocity. However, when considering droplets or bubbles of size comparable to the mean free path in the vapour, one has to consider gas rarefaction effects in the form of interfacial temperature jumps and velocity slip. In the presence of evaporation/condensation, a more or less pronounced Knudsen layer always develops, next to the liquid–vapour interface, irrespective of the curvature/size of the condensed phase surface (Sone 2000). Depending on the process (evaporation or condensation) and its intensity, more or less strong variations of macroscopic quantities occur on the scale of the mean free path (Ytrehus 1975). All such effects are well described by the Boltzmann equation, in a low-density vapour phase. Since the Boltzmann equation cannot describe the liquid phase, it has to be supplemented with a model describing the coupling of the vapour and liquid phases. Usually, the model takes the form of a *phenomenological* boundary condition, specifying the distribution function at the structureless liquid–vapour interface, as a function of a number of model parameters, typically condensation/evaporation coefficients (Frezzotti 2011). On the basis of the kinetic description, continuity of temperature and tangential velocity are replaced by more elaborate jump and slip conditions incorporating Knudsen layer effects. In many studies, particularly when dealing with intense evaporation/condensation flows, boundary condition models are used to solve the nonlinear Boltzmann equation and resolve the Knudsen layer structure (Pao 1971*a,b*; Cipolla, Lang & Loyalka 1974; Ytrehus 1975; Sone 2000).

Independent of the model – classical hydrodynamics or more elaborate theory for rarefaction – interface conditions for the distribution function and the condensation/evaporation coefficients are difficult to determine, since they can be measured not directly, but only through their effects on the flow field properties (Bond & Struchtrup 2004). The best known example for this is the evaporation/condensation coefficient of water, for which reported measurements vary by several orders of magnitude (Eames, Marr & Sabir 1997; Marek & Straub 2001). In spite of the phenomenological formulation of kinetic boundary conditions and the general difficulties in determining their parameters from comparisons with experiments, the Boltzmann equation provides a good description of the Knudsen layer structure resulting from molecular dynamics (MD) simulations of simple liquids (Frezzotti, Grosfils & Toxvaerd 2003; Barbante & Frezzotti 2017; Frezzotti & Barbante 2020) and experiments (Mager, Adomeit & Wortberg 1989; Frezzotti & Stefanov 1995). As an alternative to the direct solution of the Boltzmann equation, it is possible to derive macroscopic transport models, such as hydrodynamics or extended models, by appropriate methods, typically based on the Knudsen number as smallness parameter (Chapman & Cowling 1970; Cercignani 1975; Struchtrup 2004, 2005; Kremer 2010). Macroscopic interface conditions can be derived from the interface conditions for the Boltzmann equation within the same context (Torrilhon & Struchtrup 2008; Struchtrup *et al.* 2017; Beckmann *et al.* 2018).

The above approach to liquid–vapour flows implies a heterogeneous model that adopts Navier–Stokes–Fourier equations to describe the liquid bulk and kinetic theory to describe

kinetic effects in the vapour, at various levels. The latter provides jump formulas to bridge the hydrodynamic regions in the liquid and vapour phases across the discontinuity, resulting from collapsing the liquid–vapour interface and the adjacent Knudsen layer onto a structureless phase boundary surface (Schrage 1953; Kjelstrup & Bedeaux 2008; Caputa & Struchtrup 2011). When the Knudsen layer thickness is of the order of the curvature radius of the interface, the Navier–Stokes–Fourier equations have to be coupled to the Boltzmann equation by the kinetic boundary condition mentioned above.

Apart from direct MD simulations, a unified treatment of liquid–vapour flows by a single mathematical model is provided, for example, by diffuse interface models (DIM) (Anderson, McFadden & Wheeler 1998), in which additions of Korteweg’s capillary stress tensor to the classical Navier–Stokes contribution, and of a capillary heat flux to the classical Fourier term, allows us to describe vapour and liquid phase as classical Navier–Stokes–Fourier (NSF) fluids, connected by a diffuse interface, a few atomic diameters thick and dominated by Korteweg stresses. Unfortunately, the model reduces to the ordinary NSF equations outside the liquid–vapour interface and fails to reproduce MD evaporation/condensation rates in the dilute vapour regime (Barbante & Frezzotti 2017; Frezzotti & Barbante 2020). On the contrary, DIM perform well when the vapour becomes non-ideal, as the liquid temperature approaches the critical temperature and kinetic effects in the dense vapour fade away (Frezzotti & Barbante 2020). It is worth observing that recent results obtained from MD simulations of the Lennard-Jones fluid suggest the existence of a ‘grey’ region in which the vapour cannot be modelled by the Boltzmann equation because of its non-ideality, but DIM cannot be used because of the persistence of kinetic effects (Frezzotti & Barbante 2020).

A kinetic model for non-ideal fluids is not easily formulated (Resibois & De Leener 1977), and Enskog’s theory of dense hard-sphere fluids remains a viable model to explore kinetic effects in non-ideal gases (Enskog 1921). Its extension to fluids whose molecular potential has an attractive contribution is known as the Enskog–Vlasov (EV) equation (de Sobrino 1967). The EV equation provides a generalization of the Enskog equation to include not only dense gas effects but also phase changes. This simplified model considers binary collisions only for the repulsive hard-sphere interaction, and describes the collective attractive interaction with the sea of molecules as a self-consistent force field in the Vlasov term (Vlasov 1961). Excluded volume effects, due to the finite size of molecules, are accounted for by the non-local Enskog collision term and the presence of the pair correlation function Y (Enskog 1921; Resibois & De Leener 1977).

For equilibrium states, the EV model yields van-der-Waals-like equations of state, an easily computed liquid–vapour coexistence curve below the critical temperature and diffuse phase interfaces with surface tension (de Sobrino 1967; Grmela 1971; Frezzotti, Gibelli & Lorenzani 2005). The interface is part of the continuous solution of the EV equation, so that no additional interface conditions must be provided. In this respect, the EV model can be considered as a kinetic extension of DIM (Piechór 2008; Giovangigli 2020). Actually, just as for the Boltzmann and Enskog equations, one can derive macroscopic transport equations from the EV equation. Similarly to the EV equation itself, these macroscopic transport equations describe the continuous interface between the liquid and vapour phases, and the phases themselves, and there is no need for additional interface conditions with *ad hoc* coefficients (Piechór 2008; Giovangigli 2020).

However, the formulation of transport equations for the EV equation cannot be limited to the NSF level because of the need to describe Knudsen layers in low-density vapour flows. In this case, the EV equation reduces to the Boltzmann equation for hard spheres,

in the vapour. Hence it provides a consistent flow description, which is not possible for NSF equations. The accuracy of a hydrodynamic-like approach can be improved when higher-order terms in the Knudsen number are included in the modelling (Struchtrup 2005).

Macroscopic models at higher order are typically derived by means of Grad's method of moments, and variants thereof, which yield stable equations at any order (Grad 1949, 1958; Struchtrup 2005; Kremer 2010). This stands in contrast to the Chapman–Enskog expansion, where the higher-order Burnett (Burnett 1936) and super-Burnett (Shavaliyev 1993) equations are unstable (Bobylev 1982). The best known set of Grad-type moment equations is for 13 moments (Grad 1949), which do not exhibit any Knudsen layers (Struchtrup 2005). Indeed, modelling of all relevant contributions to Knudsen layers requires a Grad system with at least 26 moments (Struchtrup 2005). In the framework of dilute gases, a systematic reduction of the 26 moment system leads to the regularized 13 moment equations (R13) (Struchtrup & Torrilhon 2003; Struchtrup 2005; Torrilhon 2016), the simplest moment model capable of describing Knudsen layers. However, the arguments leading to the derivation of the R13 moment would not necessarily hold within interfaces, where the distribution function suffers changes on the scale of the molecular diameter. Hence in order to have macroscopic moment approximation for the EV equation that includes resolution of the interface and the Knudsen layers, we have decided to consider the 26 moments formulation – and this is what we will do in the following. The 13 moment equations for the standard Enskog equation, that is, without the Vlasov term, are available for the linearized case (Kremer & Rosa 1988). Below, we will not only consider more moments and add the Vlasov term, but also include a number of nonlinear terms that are necessary to describe the strong changes across the continuous interface. The EV equation is a nonlinear partial-integro-differential equation with non-local terms. Aiming for a macroscopic model, we will expand all non-localities into Taylor series, which will give us gradient terms in all macroscopic quantities. Due to the inherent difficulty of the derivation of moment equations for the EV equation, we consider only equations for linear deviations from an equilibrium state that involves phase interfaces. The equilibrium state exhibits homogeneous temperature, (zero) velocity, and bulk densities in vapour and liquid, but steep density gradients in the liquid–vapour interface. With that, the linearization around the equilibrium state yields seemingly nonlinear terms involving equilibrium density gradients and true non-equilibrium terms.

The present paper focuses on the derivation of the moment equations. Deeper discussion of the moment equations, as well as their solutions for a variety of problems, will be presented elsewhere. With the phase interface resolved, we hope to be able in the future to provide a rational link to the jump and slip conditions for discontinuous interfaces.

The remainder of the paper is structured as follows. The EV equation is introduced in § 2, and § 3 discusses how to obtain its moment equations and their closure by means of the Grad method. Detailed technical aspects are found in the next sections: § 4 discusses the Vlasov force and the corresponding Korteweg stress tensor, as well as the contributions to the balance of energy; evaluation of the Enskog collision term for the 26 moment closure is outlined in § 5. Non-locality is replaced by Taylor expansion, adding to the complexity – essentially a large number of integrals must be solved and combined into the moments of the collision term that are required to close the moment equations. The full set of closed 26 moment equations is presented in § 6. The paper ends with a brief discussion of the equilibrium state, a first example of a non-equilibrium solution, and our conclusions and outlook to future work on solution and discussion of the equations.

2. Enskog–Vlasov equation

The EV equation provides an approximate description of a fluid composed by identical molecules of mass m , interacting by forces directed along the line connecting their centres and determined by the Sutherland potential (Sutherland 1893)

$$\phi(r) = \begin{cases} \infty, & r < a, \\ \hat{\phi}(r), & r \geq a, \end{cases} \quad (2.1)$$

which results from the superposition of a hard-sphere repulsive core and a soft attractive tail. In (2.1), $r = \|\mathbf{x}^1 - \mathbf{x}\|$ is the distance between the centres of two molecules located respectively at \mathbf{x}^1 and \mathbf{x} . The hard-sphere diameter is denoted by a , whereas $\hat{\phi}(r)$ denotes the soft potential tail.

From the classical BBGKY hierarchy (Resibois & De Leener 1977), the following exact equation for the one-particle distribution function $f^{(1)}(\mathbf{x}, t, \mathbf{c})$ can be derived (Karkheck & Stell 1981):

$$\begin{aligned} \frac{\partial f^{(1)}}{\partial t} + c_k \frac{\partial f^{(1)}}{\partial x_k} + \frac{G_k}{m} \frac{\partial f^{(1)}}{\partial c_k} &= \frac{1}{m} \frac{\partial}{\partial c_k} \int \frac{d\hat{\phi}}{dr} \frac{x_k^1 - x_k}{\|\mathbf{x}^1 - \mathbf{x}\|} f^{(2)}(\mathbf{x}, \mathbf{c}, \mathbf{x}^1, \mathbf{c}^1, t) d\mathbf{x}^1 d\mathbf{c}^1 \\ &+ \int a^2 \left[f^{(2)}(\mathbf{x}, \mathbf{c}', \mathbf{x} + a\mathbf{k}, \mathbf{c}^1, t) - f^{(2)}(\mathbf{x}, \mathbf{c}, \mathbf{x} - a\mathbf{k}, \mathbf{c}^1, t) \right] (\mathbf{g} \cdot \mathbf{k}) H(\mathbf{g} \cdot \mathbf{k}) d^2\mathbf{k} d\mathbf{c}^1, \end{aligned} \quad (2.2)$$

where H is the Heaviside step function.

Equation (2.2) expresses the rate of change of the density of molecules in the one-particle phase space point (\mathbf{x}, \mathbf{c}) as the result of advection with velocity c_k and acceleration caused by an external body force G_k as well as of binary interactions. The latter are described by the two integrals on the right-hand side. The first integral represents the force acting on a molecule at (\mathbf{x}, \mathbf{c}) because of its interaction with any other molecule, through the soft potential tail $\hat{\phi}$. The second integral gives the rate of change of $f^{(1)}$ due to instantaneous and elastic binary collisions between two spheres whose centres are at relative distance a , at the time of their impact. The hard-spheres collision term is the sum of a loss and a gain contribution. In the former, molecules located at \mathbf{x} , with pre-collision velocity \mathbf{c} , are removed from their phase space position by collision with molecules located at $\mathbf{x} - a\mathbf{k}$, with velocity \mathbf{c}^1 . The unit vector \mathbf{k} specifies the relative position of the collision pair at the time of their impact. Upon each collision, \mathbf{c} and \mathbf{c}^1 are transformed into the respective post-collision velocities \mathbf{c}' and $\mathbf{c}^{1'}$, according to the expressions

$$\mathbf{c}' = \mathbf{c} + (\mathbf{g} \cdot \mathbf{k})\mathbf{k}, \quad \mathbf{c}^{1'} = \mathbf{c}^1 - (\mathbf{g} \cdot \mathbf{k})\mathbf{k}, \quad \mathbf{g} = \mathbf{c}^1 - \mathbf{c}. \quad (2.3a-c)$$

The gain term is obtained by considering ‘inverse’ collisions in which collision pairs respectively occupy positions \mathbf{x} and $\mathbf{x} + a\mathbf{k}$, having pre-collision velocities \mathbf{c}' and $\mathbf{c}^{1'}$ that transform into post-collision velocities \mathbf{c} and \mathbf{c}^1 , as seen easily from (2.3a–c). For both contributions, the integration is carried over all \mathbf{k} and \mathbf{c}^1 such that the flux $(\mathbf{g} \cdot \mathbf{k}) H(\mathbf{g} \cdot \mathbf{k})$ across the unit sphere element is positive (impacting molecules are approaching each other). It should be noted that in both binary interaction terms, the two-particle distribution function has to be used, since the exact evaluation of the corresponding terms requires the knowledge of pair distributions, not available from $f^{(1)}$ alone.

Truncating the hierarchy at the level of $f^{(1)}$ requires assumptions about pair correlations. The EV equation, first obtained by de Sobrino in 1967 (de Sobrino 1967), adopts

Enskog's (Enskog 1921) approximation of the hard-sphere contribution, while ignoring pair correlations in the potential tail term. More precisely, in the second integral on the right-hand side of (2.2), the pair distribution function at contact is written as

$$\left. \begin{aligned} f^{(2)}(\mathbf{x}, \mathbf{c}, \mathbf{x} - a\mathbf{k}, \mathbf{c}^1, t) &= \chi_{hs}(\mathbf{x}, \mathbf{x} - a\mathbf{k} | n) f^{(1)}(\mathbf{x}, \mathbf{c}, t) f^{(1)}(\mathbf{x} - a\mathbf{k}, \mathbf{c}^1, t), \\ f^{(2)}(\mathbf{x}, \mathbf{c}', \mathbf{x} + a\mathbf{k}, \mathbf{c}^{1'}, t) &= \chi_{hs}(\mathbf{x}, \mathbf{x} + a\mathbf{k} | n) f^{(1)}(\mathbf{x}, \mathbf{c}', t) f^{(1)}(\mathbf{x} + a\mathbf{k}, \mathbf{c}^{1'}, t). \end{aligned} \right\} \quad (2.4)$$

In the original Enskog formulation of the dense hard-sphere gas (Enskog 1921), named standard Enskog theory (SET), the assumed velocity-independent pair correlation function χ_{hs} is assigned as a function of the fluid number density n from the uniform-equilibrium pair correlation function $Y(n)$ at the contact position $\mathbf{x} \mp (a/2)\mathbf{k}$. Hence the SET approximation of the hard-sphere contribution in (2.2) takes the form

$$\begin{aligned} S_{En} &= a^2 \int \int_0^{2\pi} \int_0^{\pi/2} \left\{ \begin{aligned} &Y \left[n \left(\mathbf{x} + \frac{a\mathbf{k}}{2} \right) \right] f(\mathbf{x} + a\mathbf{k}, \mathbf{c}^1) f(\mathbf{x}, \mathbf{c}') \\ &- Y \left[n \left(\mathbf{x} - \frac{a\mathbf{k}}{2} \right) \right] f(\mathbf{x} - a\mathbf{k}, \mathbf{c}^1) f(\mathbf{x}, \mathbf{c}) \end{aligned} \right\} \\ &\times g \cos \theta \sin \theta \, d\theta \, d\varepsilon \, d\mathbf{c}^1, \end{aligned} \quad (2.5)$$

where $\mathbf{k} = \{\cos \varepsilon \sin \theta, \sin \varepsilon \sin \theta, \cos \theta\}$.

A further assumption about pair correlations is added to simplify the soft tail contribution, where $f^{(2)}$ is written as

$$f^{(2)}(\mathbf{x}, \mathbf{c}, \mathbf{x}^1, \mathbf{c}^1, t) = f^{(1)}(\mathbf{x}, \mathbf{c}, t) f^{(1)}(\mathbf{x}^1, \mathbf{c}^1, t), \quad (2.6)$$

thus ignoring position and velocity correlations when pair distance is larger than the range of repulsive forces. Taking into account (2.6), the soft potential tail contribution in (2.2) takes the form of a Vlasov-like (Vlasov 1961) self-consistent force field given by

$$F_k(x_l) = \int_{\|\mathbf{x}^1 - \mathbf{x}\| > a} \frac{d\phi}{dr} \frac{x_k^1 - x_k}{\|\mathbf{x}^1 - \mathbf{x}\|} n(x_j^1) \, d\mathbf{x}^1, \quad (2.7)$$

which determines the force acting on a molecule at position \mathbf{x} and time t as a non-local linear functional of the number density field n .

Within the assumptions listed above, the EV equation reads (now in index notation that will be used in most of what follows)

$$\frac{\partial f}{\partial t} + c_k \frac{\partial f}{\partial x_k} + [F_k(x_l) + G_k] \frac{\partial f}{\partial c_k} = S_{En}. \quad (2.8)$$

From the physical point of view, (2.8) describes a hard-sphere fluid, subject to a self-consistent force field determined by the attractive part of the potential ϕ . Unlike the Boltzmann equation (Cercignani 1975), which describes dilute gases, its approximate one-particle distribution function extension to dense fluids requires a model for pair correlations. In the framework of SET, a relationship between the uniform-equilibrium pair correlation function $Y(n)$ and the pressure equation of state is easily established, in

the form of a generalized van der Waals equation (Balescu 1975), as

$$\left. \begin{aligned} p(n, T) &= p_{hs}(n, T) - \alpha_t n^2, \\ p_{hs}(n, T) &= nk_B T \left[1 + \frac{2\pi}{3} a^3 n Y(n) \right], \end{aligned} \right\} \quad (2.9)$$

where p_{hs} is the hard-sphere term contribution and α_t is a coefficient depending on $\hat{\phi}$. As shown by Frezzotti, Barbante & Gibelli (2019), the critical density n_{crit} of the EV fluid in equilibrium is determined only by the hard-sphere potential, through the assumed Y function. In contrast to this, the critical temperature, T_{crit} depends as well on the soft potential tail $\hat{\phi}(r)$. Since in this work it is not necessary to tune $Y(n)$ and α_t on a specific fluid, it has been decided to derive $Y(n)$ from the Carnahan–Starling hard-sphere fluid equation of state (Carnahan & Starling 1969), as

$$Y[n] = \frac{1}{2} \frac{2 - \eta}{(1 - \eta)^3}, \quad (2.10)$$

where $\eta = \pi a^3 n / 6$ is the fluid reduced density. It is to be noted that the Carnahan–Starling equation provides a very accurate approximation of the hard-sphere equation of state, up to a reduced density of about 0.4, where the hard-sphere fluid suffers a liquid–solid phase transition (Balescu 1975). The attracting part of the potential has been chosen as a power potential of order γ ,

$$\hat{\phi}(r) = -\phi_a \left(\frac{a}{r} \right)^\gamma, \quad (2.11)$$

with $\gamma = 6$, in order to mimic the attractive contribution of the Lennard-Jones potential (Jones 1924).

The brief description of the assumptions leading to (2.8) clearly show its phenomenological nature. Over the years, several studies have addressed correcting some of its deficiencies. In particular, van Beijeren and Ernst (Van Beijeren & Ernst 1973) have proposed replacing the local uniform-equilibrium pair correlation function Y with the exact pair correlation function of a hard-sphere fluid in non-uniform equilibrium, $\chi(\mathbf{r}, \mathbf{r} \mp \mathbf{k} | n)$. The latter, unlike $Y(n)$, is a non-local functional of the density, formally defined by a cluster expansion (Van Beijeren & Ernst 1973; Balescu 1975) and difficult to use in applications. Yet the resulting revised Enskog theory (RET) has several advantages over SET. First, RET becomes exact when the hard-sphere fluid is in equilibrium with an arbitrary density field. Second, RET extension to mixtures makes it compatible with irreversible thermodynamics, whereas SET is not (Van Beijeren & Ernst 1973). Third, the H-theorem has not been proved for SET, whereas a proof is available for RET (Resibois 1978). The modifications of Enskog’s theory mentioned above are related to Enskog’s hard-sphere term in (2.8); a discussion of the theoretical properties of the extension to the EV equation can be found in Benilov & Benilov (2018).

In spite of the improved formulations mentioned above, in this paper the original SET form of the hard-sphere interaction contribution has been used, for various reasons. First, the derivation of the moment equations described below is rather complex, and the use of the simpler SET does not add further difficulties. Moreover, previous results (Kremer 2010) that limited Grad’s 13 moment formulation of the Enskog equation are available for comparisons and cross-checks. Second, in spite of its theoretical drawbacks, numerical solutions of the SET version of the Enskog equation have shown very good agreement

with exact molecular dynamics simulations of the dense hard-sphere fluid, for highly non-equilibrium flows (Frezzotti 1998, 1999). When the self-consistent Vlasov field is added to simulate two-phase flows, computed evaporation coefficients and flow fields compare very well to molecular dynamics simulations (Frezzotti *et al.* 2005).

3. Transport equations for 26 moments

3.1. Definition of moments

Moments are weighted averages of the distribution function, some of which have direct physical meaning, such as the mass density ρ , or the bulk velocity v_i . Following Struchtrup (2005), we consider the usual central moments of the distribution function defined as

$$u_{\langle i_1 \dots i_n \rangle}^\alpha = m \int C^{2\alpha} C_{\langle i_1} \dots C_{i_n \rangle} f \, dc, \tag{3.1}$$

where $C_i = c_i - v_i$ is the peculiar velocity and m is particle mass; indices between angular brackets indicate trace-free and symmetric tensors. Experience from the Boltzmann equation (Struchtrup 2005; Torrilhon 2016) shows that the following 26 variables serve well to describe gas flows at not too large Knudsen numbers:

$$\left. \begin{aligned} \rho &= mn = u^0, \\ \rho v_i &= m \int c_i f \, dc, \\ \rho \epsilon &= \frac{3}{2} \rho RT = \frac{3}{2} \rho \theta = \frac{1}{2} u^2, \\ \sigma_{ij} &= u_{\langle ij \rangle}^0, \\ q_i &= \frac{1}{2} u_i^1, \\ m_{ijk} &= u_{\langle ijk \rangle}^0, \\ \Delta &= u^4 - 15 \rho \theta^2, \\ R_{ij} &= u_{\langle ij \rangle}^1 - 7 \theta \sigma_{ij}. \end{aligned} \right\} \tag{3.2}$$

Above, for the first five moments, ρ , ρv_i and $\rho \epsilon$ are mass density, momentum density, and density of thermal energy, where $\theta = RT$ is the temperature in units of specific energy, $R = k_B/m$ is the gas constant, k_B is the Boltzmann constant, and T is thermodynamic temperature. The other variables are all non-equilibrium moments, that is, they vanish in equilibrium states. Stress tensor σ_{ij} and heat flux q_i are the kinetic contributions to overall stress and energy flux; there will be additional contributions from the Enskog and Vlasov terms that will emerge further below. The order of magnitude method for classical rarefied gas dynamics for Maxwell molecules shows that stress and heat flux are of first order in the Knudsen number, while the variables m_{ijk} , Δ and R_{ij} are constructed to be of second order (Struchtrup 2004, 2005). Since we expect a close relationship between moment equations from the EV theory and classical kinetic theory, we prefer to use the same variables.

3.2. Grad distribution function

Moment equations result from multiplying the kinetic equation with appropriate tensor combinations of microscopic velocity, and integration. The moment equations are coupled,

since higher moments always appear under space derivatives. When one has chosen a certain set of moments as variables, the corresponding set of moment equations contains higher moments that must be related somehow to the chosen variables. In the Grad method, this closure problem is solved by constructing a distribution function that reproduces the variables, and allows us to determine all other moments through the variables (Grad 1949, 1958; Struchtrup 2005; Kremer 2010).

Just as for the Boltzmann equation, the Grad distribution is constructed as a deviation from a local Maxwellian, whose macroscopic parameters coincide with the corresponding moments of f . With the 26 moments listed above, closure is performed by the 26 moment distribution function (Struchtrup 2005), which reads

$$f|_{26} = \hat{f}_M (\rho + \Phi), \tag{3.3}$$

with the reduced Maxwellian

$$\hat{f}_M = \frac{1}{m\sqrt{2\pi\theta^3}} e^{-(C^2/2\theta)}, \tag{3.4}$$

and the non-equilibrium deviation Φ expressed as a polynomial in the peculiar velocity,

$$\begin{aligned} \Phi = & \frac{\sigma_{ij}}{2\theta^2} C_{(i} C_{j)} + \frac{2}{5} \frac{q_k}{\theta^2} C_k \left(\frac{C^2}{2\theta} - \frac{5}{2} \right) \\ & + \frac{m_{ijk}}{6\theta^3} C_{(i} C_j C_{k)} + \frac{R_{ij}}{14\theta^3} C_{(i} C_{j)} \left(\frac{C^2}{2\theta} - \frac{7}{2} \right) + \frac{\Delta}{8\theta^2} \left(1 - \frac{2}{3} \frac{C^2}{\theta} + \frac{1}{15} \frac{C^4}{\theta^2} \right). \end{aligned} \tag{3.5}$$

Here, the first two terms correspond to Grad’s classical 13 moments closure. In equilibrium, all higher moments vanish, $0 = \Delta = q_k = \sigma_{ij} = R_{ij} = m_{ijk}$, hence the equilibrium solution is the Maxwellian $f_M = \rho \hat{f}_M$. More precisely, it is worth observing that the equilibrium solution of the EV equation is a Maxwell distribution function with uniform θ and \mathbf{v} . Depending on the equilibrium value of θ , the equilibrium density ρ is not generally uniform, obeying an integral equation expressing the local balance of mean field and hard-sphere pressure tensor contributions. Also, for later reference, we emphasize that the non-equilibrium correction Φ is independent of mass density.

This distribution (3.3) reproduces the 26 moments of the theory (see (3.2)), and the higher moments required for closure are determined as (Struchtrup 2005)

$$u_{i|26}^2 = 28\theta q_i, \quad u_{ijk|26}^1 = 9\theta m_{ijk}, \quad u_{ijkl|26}^0 = 0. \tag{3.6a-c}$$

This distribution will also be used for determining the Enskog production terms, which result from taking appropriate moments of the collision term.

A distribution function should be positive. Due to its polynomial structure, for the Grad approximation this is not the case, since Φ becomes negative for large values of C_i . For not too large values of the moments in (3.5), the multiplying Maxwellian in (3.3) suppresses these negative values, and the resulting equations remain meaningful.

The entropy inequality – also known as the H-theorem – results from integration of the kinetic equation against $\ln f$, which does not exist for the Grad distribution, due to the non-positivity. Evaluation of the entropy therefore must rely on Taylor expansion of $\ln \Phi$ in terms of the moments. This implies that for Grad-type moment equations, an H-theorem can be only approximated, but not guaranteed for all values of the moments. One can show that fully linearized Grad equations as derived from the Boltzmann equation are accompanied by a quadratic entropy; see Struchtrup & Torrilhon (2007).

While an H-theorem for nonlinear moment equations cannot be proved, Grad-type moment equations remain stable and give meaningful results also outside the linear regime; e.g. see the review by Torrilhon (2016). The same behaviour is expected from the moment equations derived below. An examination of the accompanying H-theorem, at least for the fully linearized equations, is planned for the future.

3.3. Moment equations

3.3.1. General form

Moment equations are formed by multiplying the kinetic equation with the appropriate polynomial in velocity, and subsequent integration. The general moment equation for arbitrary moments (3.1) was presented in Struchtrup (2005) for the Boltzmann equation. Since EV differs only in the Vlasov force and the details of the collision term, we can take the general moment equation from Struchtrup (2005), add the Vlasov force F_k , and keep the general notation for production terms, so that

$$\begin{aligned} & \frac{D u_{i_1 \dots i_n}^\alpha}{Dt} + 2\alpha u_{i_1 \dots i_n k}^{\alpha-1} \left[\frac{D v_k}{Dt} - F_k - G_k \right] \\ & + \frac{n(2\alpha + 2n + 1)}{2n + 1} u_{(i_1 \dots i_{n-1}}^\alpha \left[\frac{D v_{i_n}}{Dt} - F_{i_n} - G_{i_n} \right] \\ & + \frac{\partial u_{i_1 \dots i_n k}^\alpha}{\partial x_k} + \frac{n}{2n + 1} \frac{\partial u_{(i_1 \dots i_{n-1}}^{\alpha+1}}{\partial x_{i_n}} + 2\alpha u_{i_1 \dots i_n k l}^{\alpha-1} \frac{\partial v_k}{\partial x_l} \\ & + 2\alpha \frac{n + 1}{2n + 3} u_{(i_1 \dots i_n}^\alpha \frac{\partial v_k}{\partial x_k} + 2\alpha \frac{n}{2n + 1} u_{k(i_1 \dots i_{n-1}}^\alpha \frac{\partial v_k}{\partial x_{i_n}} + n u_{k(i_1 \dots i_{n-1}}^\alpha \frac{\partial v_{i_n}}{\partial x_k} \\ & + u_{i_1 \dots i_n}^\alpha \frac{\partial v_k}{\partial x_k} + \frac{n(n - 1)}{4n^2 - 1} (2\alpha + 2n + 1) u_{(i_1 \dots i_{n-2}}^{\alpha+1} \frac{\partial v_{i_{n-1}}}{\partial x_{i_n}} = \mathcal{P}_{i_1 \dots i_n}^\alpha. \end{aligned} \tag{3.7}$$

Here, $D/Dt = \partial/\partial t + v_k(\partial/\partial x_k)$ is the convective time derivative, G_i is the external body force, e.g. from gravity, and F_i is the Vlasov force from above. The so-called production terms on the right-hand side are integrals over the Enskog collision term,

$$\mathcal{P}_{i_1 \dots i_n}^\alpha = m \int C^{2\alpha} C_{(i_1} \dots C_{i_n)} \mathcal{S}_{En} dc. \tag{3.8}$$

The general moment equation contains time derivatives of velocity that enter through derivatives of the peculiar velocity $C_i = c_i - v_i$; the balance of momentum will be used to replace these contributions. Equations for particular moments follow by choice of particular values of the velocity power α and the tensor rank n , and replacing moments $u_{(i_1 \dots i_n)}^\alpha$ through the variables listed in (3.2). Details of the Vlasov force and production terms will be discussed in later sections.

3.3.2. Conservation laws

We begin with the conservation laws, in which we have to write production terms for energy and momentum, since there will be flux contributions (in divergence form for the full conservation laws) from the Enskog terms for momentum and energy. This accounts for the fact that in a hard-sphere collision, energy and momentum are transferred over the distance of the colliding particles' centre of mass. Since mass is not transferred between

the particles, so that there is no production of mass, $m \int \mathcal{S}_{En} \, d\mathbf{c} = 0$, and the production of momentum is $m \int c_i \mathcal{S}_{En} \, d\mathbf{c} = m \int C_i \mathcal{S}_{En} \, d\mathbf{c} = \mathcal{P}_i^0$.

The conservation laws for mass and momentum, and the balance of thermal energy, read

$$\left. \begin{aligned} \frac{D\rho}{Dt} + \rho \frac{\partial v_k}{\partial x_k} &= 0, \\ \rho \frac{Dv_i}{Dt} + \frac{\partial \rho \theta}{\partial x_i} + \frac{\partial \sigma_{ik}}{\partial x_k} &= \rho (F_i + G_i) + \mathcal{P}_i^0, \\ \frac{3}{2} \rho \frac{D\theta}{Dt} + \frac{\partial q_k}{\partial x_k} &= -\rho \theta \frac{\partial v_k}{\partial x_k} - \sigma_{kl} \frac{\partial v_k}{\partial x_l} + \frac{1}{2} \mathcal{P}^1. \end{aligned} \right\} \quad (3.9)$$

Here, and further below, we removed the velocity time derivative from (3.7) by means of the momentum balance, which also removes the contributions of external body force and Vlasov force. Hence the force terms will appear only in the momentum balance, but not in the other equations for central moments.

3.3.3. Balance for Δ

The conservation laws are used to simplify the equations for other variables, by eliminating the time derivative of velocity, and use of the energy equation and mass balance where required. We proceed through several tensor orders, beginning here with the scalar equation for $\Delta = u^2 - 15\rho\theta^2$, which requires not only the moment equation for u^2 , but also mass and energy balances to eliminate time derivatives of $15\rho\theta^2$. Omitting all detail of computation, we simply state the final result, based on the 26 moments closure (3.3). We obtain the same equation as in Struchtrup (2005), only with additional terms in the production, which come from the Enskog contributions to energy and momentum and will be discussed later:

$$\begin{aligned} \frac{D\Delta}{Dt} + 8\theta \frac{\partial q_k}{\partial x_k} + 8\theta \sigma_{kl} \frac{\partial v_k}{\partial x_l} + 20q_k \frac{\partial \theta}{\partial x_k} - 8q_k \theta \frac{\partial \ln \rho}{\partial x_k} - \frac{8q_k}{\rho} \frac{\partial \sigma_{kl}}{\partial x_l} + 4R_{kl} \frac{\partial v_k}{\partial x_l} + \frac{7}{3} \Delta \frac{\partial v_k}{\partial x_k} \\ = \mathcal{P}^2 - 20\theta \frac{\mathcal{P}^1}{2} - \frac{8q_k}{\rho} \mathcal{P}_k^0. \end{aligned} \quad (3.10)$$

3.3.4. Balance for q_i

The equation for the kinetic contribution to energy flux, q_i , is the same as in standard kinetic theory (Struchtrup 2005), except that the Enskog term yields additional production terms:

$$\begin{aligned} \frac{Dq_i}{Dt} + \frac{5}{2} \rho \theta \frac{\partial \theta}{\partial x_i} + \frac{5}{2} \sigma_{ik} \frac{\partial \theta}{\partial x_k} + \theta \frac{\partial \sigma_{ik}}{\partial x_k} - \sigma_{ik} \theta \frac{\partial \ln \rho}{\partial x_k} + \frac{7}{5} q_k \frac{\partial v_i}{\partial x_k} + \frac{2}{5} q_k \frac{\partial v_k}{\partial x_i} + \frac{7}{5} q_i \frac{\partial v_k}{\partial x_k} \\ + \frac{1}{2} \frac{\partial R_{ik}}{\partial x_k} + \frac{1}{6} \frac{\partial \Delta}{\partial x_i} + m_{ikl} \frac{\partial v_k}{\partial x_l} - \frac{\sigma_{ik}}{\rho} \frac{\partial \sigma_{kl}}{\partial x_l} = \frac{1}{2} \mathcal{P}_i^1 - \frac{5}{2} \theta \mathcal{P}_i^0 - \frac{\sigma_{ik}}{\rho} \mathcal{P}_k^0. \end{aligned} \quad (3.11)$$

3.3.5. Balances for σ_{ij} and R_{ij}

Also, the balances for stress σ_{ij} and the variable R_{ij} agree with results in (Struchtrup 2005), except that additional production terms appear. We find

$$\frac{D\sigma_{ij}}{Dt} + 2\rho\theta \frac{\partial v_{(i}}{\partial x_{j)}} + \sigma_{ij} \frac{\partial v_k}{\partial x_k} + \frac{4}{5} \frac{\partial q_{(i}}{\partial x_{j)}} + 2\sigma_{k(i} \frac{\partial v_{j)}}{\partial x_k} + \frac{\partial m_{ijk}}{\partial x_k} = \mathcal{P}_{ij}^0, \quad (3.12)$$

and with the trace-free velocity gradient $S_{ij} = \partial v_{(i}/\partial x_{j)}$,

$$\begin{aligned} & \frac{DR_{ij}}{Dt} + \frac{28}{5}\theta \frac{\partial q_{\langle i}}{\partial x_{j)}} + \frac{28}{5}q_{\langle i} \frac{\partial \theta}{\partial x_{j)}} - \frac{28}{5}\theta q_{\langle i} \frac{\partial \ln \rho}{\partial x_{j)}} - \frac{28}{5} \frac{q_{\langle i}}{\rho} \frac{\partial \sigma_{j)l}}{\partial x_l} + 8\sigma_{k\langle i}S_{j)k} \\ & - \frac{14}{3} \frac{\sigma_{ij}}{\rho} \frac{\partial q_k}{\partial x_k} - \frac{14}{3} \frac{\sigma_{ij}\sigma_{kl}}{\rho} \frac{\partial v_k}{\partial x_l} + \frac{14}{15}\Delta \frac{\partial v_{(i}}{\partial x_{j)}} - \frac{2m_{ijk}}{\rho} \frac{\partial \sigma_{kl}}{\partial x_l} - 2m_{ijk}\theta \frac{\partial \ln \rho}{\partial x_k} \\ & + 7m_{ijk} \frac{\partial \theta}{\partial x_k} + 2\theta \frac{\partial m_{ijk}}{\partial x_k} + \frac{8}{7}R_{k\langle i}S_{j)k} + 2R_{k\langle i} \frac{\partial v_k}{\partial x_{j)}} + \frac{5}{3}R_{ij} \frac{\partial v_k}{\partial x_k} \\ & = \mathcal{P}_{ij}^1 - 7\theta \mathcal{P}_{ij}^0 - \frac{14}{3} \frac{\sigma_{ij}}{\rho} \frac{\mathcal{P}^1}{2} - 2 \frac{m_{ijk}}{\rho} \mathcal{P}_k^0 - \frac{28}{5} \frac{q_{\langle i}}{\rho} \mathcal{P}_{j)k}^0. \end{aligned} \tag{3.13}$$

3.3.6. Balance for m_{ijk}

Finally, for the third moment we find

$$\begin{aligned} & \frac{Dm_{ijk}}{Dt} + 3\theta \frac{\partial \sigma_{\langle ij}}{\partial x_{k)}} - 3\theta \sigma_{\langle ij} \frac{\partial \ln \rho}{\partial x_{k)}} + \frac{12}{5}q_{\langle i} \frac{\partial v_{j)}}{\partial x_{k)}} - \frac{3\sigma_{\langle ij}}{\rho} \frac{\partial \sigma_{k)l}}{\partial x_l} + \frac{3}{7} \frac{\partial R_{\langle ij}}{\partial x_{k)}} \\ & + 3m_{l\langle ij} \frac{\partial v_{k)}}{\partial x_l} + m_{ijk} \frac{\partial v_l}{\partial x_l} = \mathcal{P}_{ijk}^0 - \frac{3\sigma_{\langle ij}}{\rho} \mathcal{P}_{k)k}^0. \end{aligned} \tag{3.14}$$

4. Vlasov force

4.1. Smooth density approximation

As shown in (2.7), the Vlasov force F_k depends solely on the density distribution of the particles, independent of their velocities. Therefore, the full distribution function f is not required for its computation. Assuming that the number density n is sufficiently smooth anywhere, including at the phase interface, we can expand the number density in the integral, so that

$$F_k(x_l) = \frac{\partial n}{\partial x_s} \int_{r>a} \frac{d\phi}{dr} \frac{r_k r_s}{r} dr + \frac{1}{6} \frac{\partial^3 n}{\partial x_r \partial x_s \partial x_t} \int_{r>a} \frac{d\phi}{dr} \frac{r_k r_r r_s r_t}{r} dr, \tag{4.1}$$

where $r_k = x_k^1 - x_k$ is the distance vector between the interacting particles, and we have switched integration variables (with $x_k^1 = x_k + r_k$, we find $dx dx^1 = dx dr$); anisotropic contributions of the integrals vanish, since we integrate over a sphere.

Integration yields the Vlasov force in the form

$$F_k(x_l) = \frac{4\pi a^3}{3} \frac{\phi_a}{m} \chi_1 \frac{\partial \rho}{\partial x_k} + \frac{2\pi a^5}{15} \frac{\phi_a}{m} \chi_3 \frac{\partial^3 \rho}{\partial x_k \partial x_s \partial x_s}, \tag{4.2}$$

where for power potentials

$$\chi_1 = \frac{\gamma}{\gamma - 3}, \quad \chi_3 = \frac{\gamma}{\gamma - 5}, \tag{4.3a,b}$$

and for the exponential tail

$$\chi_1 = \frac{6}{\varphi^3} + \frac{6}{\varphi^2} + \frac{3}{\varphi} + 1, \quad \chi_3 = \frac{120}{\varphi^5} + \frac{120}{\varphi^4} + \frac{60}{\varphi^3} + \frac{20}{\varphi^2} + \frac{5}{\varphi} + 1. \tag{4.4a,b}$$

4.2. Korteweg stress tensor

In the balance of momentum, the Vlasov force F_k is multiplied by mass density ρ . It is a simple exercise to rewrite the force term as the divergence of the potential tail contribution to the Korteweg stress tensor, i.e.

$$\rho F_k = -\frac{\partial \mathcal{T}_{ks}^K}{\partial x_s}, \quad (4.5)$$

with

$$\mathcal{T}_{ks}^K = -\frac{2\pi a^3}{3} \frac{\phi_a}{m} \chi_1 \rho^2 \delta_{ks} - \frac{2\pi a^5}{15} \frac{\phi_a}{m} \chi_3 \left[\left(\rho \frac{\partial^2 \rho}{\partial x_r \partial x_r} + \frac{1}{2} \frac{\partial \rho}{\partial x_r} \frac{\partial \rho}{\partial x_r} \right) \delta_{ks} - \frac{\partial \rho}{\partial x_s} \frac{\partial \rho}{\partial x_k} \right]. \quad (4.6)$$

The first term is a van-der-Waals-like contribution describing pressure reduction through attractive forces, and the second term describes extra stress due to density gradients, including surface tension effects in phase interfaces (Anderson *et al.* 1998).

4.3. Korteweg/Vlasov energy

The potential energy due to the attractive forces between particles is a contribution to the overall energy, and appears in the overall energy balance. Energy for the Korteweg stresses has a van-der-Waals-like contribution and a contribution due to density gradients (Anderson *et al.* 1998)

$$\epsilon_K = -\frac{2\pi a^3}{3} \frac{\phi_a}{m} \chi_1 \rho + \frac{\pi a^5}{15} \frac{\phi_a}{m} \chi_3 \frac{1}{\rho} \frac{\partial \rho}{\partial x_s} \frac{\partial \rho}{\partial x_s}, \quad (4.7)$$

which obeys the non-conservation law

$$\rho \frac{D\epsilon_K}{Dt} + \frac{\partial q_k^K}{\partial x_k} = -\mathcal{T}_{rs}^K \frac{\partial v_r}{\partial x_s}, \quad (4.8)$$

where

$$q_i^K = \frac{2\pi a^5}{15} \frac{\phi_a}{m} \chi_3 \rho \frac{\partial \rho}{\partial x_i} \frac{\partial v_r}{\partial x_r} \quad (4.9)$$

is an extra contribution to energy flux (Giovangigli 2020).

The balance of kinetic energy results from multiplying the momentum balance with velocity:

$$\rho \frac{D\frac{1}{2}v^2}{Dt} + \frac{\partial(\rho\theta\delta_{ik} + \sigma_{ik} + \mathcal{T}_{ik}^K)v_i}{\partial x_k} = (\rho\theta\delta_{ik} + \sigma_{ik} + \mathcal{T}_{ik}^K) \frac{\partial v_i}{\partial x_k} + \rho v_i G_i + v_i \mathcal{P}_i^0. \quad (4.10)$$

Adding balances for thermal (third equation of the set (3.9)), potential (4.8) and kinetic (4.10) energies yields the balance of total energy in intermediate form:

$$\begin{aligned} & \rho \frac{D\left(\frac{3}{2}\theta + \frac{1}{2}v^2 + \epsilon_K\right)}{Dt} + \frac{\partial [q_k + q_k^K + (\rho\theta\delta_{ik} + \sigma_{ik} + \mathcal{T}_{ik}^K)v_i]}{\partial x_k} \\ & = \rho v_i G_i + \frac{1}{2} \mathcal{P}^1 + v_i \mathcal{P}_i^0. \end{aligned} \quad (4.11)$$

The energy balance still contains the energy and momentum contributions from the Enskog collision term, which will turn out to be of divergence form (Resibois & De Leener 1977), that is, these are additional contributions to stress and heat flux.

5. Enskog collision term

The last – and major – step in the derivation of higher-order macroscopic equations for the EV equation is finding explicit expressions for the collision productions

$$\mathcal{P}_{i_1 \dots i_n}^\alpha = m \int C^{2\alpha} C_{(i_1} \dots C_{i_n)} \mathcal{S}_{En} \, dc \tag{5.1}$$

from the Enskog collision term \mathcal{S}_{En} (see (2.5)).

Evaluation of the Enskog collision term for the Grad closure is, in principle, straightforward, but extremely cumbersome. The non-localities are replaced by Taylor series in space, which leads to a large number of individual contributions to the collision integrals. We aim to provide sufficient detail, but omit most intermediate steps. For the calculations, we mixed integration through appropriate software packages (Wolfram Mathematica™) with calculations by hand. The final results of this section are the collision terms for the transport equations (3.10)–(3.14).

The presentation in this section is rather technical, and aims to show the many steps that one has to go through to find the final expressions used. Readers not interested in computational detail are welcome to skip forward, and just study the resulting equations as presented in § 6.

5.1. Moment productions

We write in compact notation

$$P_\psi = \int \psi(c) \mathcal{S}_{En} \, dc. \tag{5.2}$$

Due to symmetry of collision details, we can use the same standard arguments on exchange and renaming of integration variables as for the Boltzmann equation (Struchtrup 2005; Kremer 2010) to compact the expression for the production terms into

$$\begin{aligned} \mathcal{P}_\psi &= a^2 \int \int \int_0^{2\pi} \int_0^{\pi/2} \{\psi' - \psi\} Y \left[n \left(x_r - \frac{ak_r}{2} \right) \right] f(x_s - ak_s, c_s^1) f(x_t, c_t) \\ &\quad \times g \cos \theta \sin \theta \, d\theta \, d\varepsilon \, dc^1 \, dc, \end{aligned} \tag{5.3}$$

where $\psi' = \psi(c')$. Apart from the non-localities in the arguments of n and f , this agrees with (3.18) in Struchtrup (2005) for the Boltzmann equation. The production term for the mass balance is obtained for $\psi(c) = m$, so that $\psi' - \psi = 0$, hence we see immediately that mass is conserved, $\mathcal{P}_m = \mathcal{P}^0 = 0$, as anticipated above.

The last step is insertion of the Grad distribution (3.3) into (5.3), and evaluation of the integral. We need to integrate over the collision vector $\mathbf{k} = \{\cos \varepsilon \sin \theta, \sin \varepsilon \sin \theta, \cos \theta\}$, which occurs in the non-local argument of n and f . To make this integration accessible, we perform expansions of the functions $Y[n(x_r - ak_r/2)]$ and $f(x_s - ak_s, c_s^1)$ around the point \mathbf{x} , as outlined in the following subsections. As noted by Frezzotti *et al.* (2005), it is necessary to retain terms up to a^5 in the Vlasov force, in order to obtain the correct soft tail contribution to the Korteweg capillary stress tensor. In the production terms, we have already the factor a^2 in front, hence, for consistency, we expand the integrand up to third-order terms in a .

5.2. Expansion of correlation function

We expand the function $Y[n(x_r - ak_r/2)]$. The Taylor series around $n(x_r)$ reads

$$Y \left[n \left(x_r - \frac{ak_r}{2} \right) \right] \simeq Y - Y_r ak_r + Y_{rs} a^2 k_r k_s - Y_{rst} a^3 k_r k_s k_t, \quad (5.4)$$

with

$$Y = Y[n(x_r)], \quad Y_r = \frac{1}{2} \frac{\partial Y}{\partial x_r}, \quad Y_{rs} = \frac{1}{8} \frac{\partial^2 Y}{\partial x_r \partial x_s}, \quad Y_{rst} = \frac{1}{48} \frac{\partial^3 Y}{\partial x_r \partial x_s \partial x_t}, \quad (5.5a-d)$$

where Y_{rs} and Y_{rst} are fully symmetric.

5.3. Expansion of the distribution function

Also, the expansion of the distribution function is, in principle, straightforward:

$$f(x_s - ak_s, c_s) = f - \frac{\partial f}{\partial x_u} ak_u + \frac{1}{2} \frac{\partial^2 f}{\partial x_u \partial x_v} a^2 k_u k_v - \frac{1}{6} \frac{\partial^3 f}{\partial x_u \partial x_v \partial x_w} a^3 k_u k_v k_w. \quad (5.6)$$

To proceed, we have to insert $f_{|26}$ from (3.3) and consider the derivatives carefully. Since $f_{|26}$ depends explicitly on the 26 variables $\{\rho, v_i, \theta, \Delta, \sigma_{ij}, q_i, R_{ij}, m_{ijk}\}$, the derivatives of $f_{|26}$ give rise to a large number of linear and nonlinear terms. We will aim for a mainly linear theory, and ignore all nonlinear terms in the non-equilibrium moments and the derivatives of all variables, except density. Density changes strongly over the equilibrium phase interface, and its gradient terms appear in the Vlasov force. For consistency, we have to have the same level of density gradient terms in the Enskog contributions. However, from (3.3), where the non-equilibrium contribution ϕ is independent of density, it is clear that $f_{|26}$ is linear in mass density.

From (3.3), for the first derivative of $f_{|26}$ we have

$$\frac{\partial f_{|26}}{\partial x_u} = \frac{\partial \hat{f}_M}{\partial x_u} (\rho + \Phi) + \hat{f}_M \left(\frac{\partial \rho}{\partial x_u} + \frac{\partial \Phi}{\partial x_u} \right), \quad (5.7)$$

where

$$\frac{\partial \hat{f}_M}{\partial x_u} = \hat{f}_M \left[\left(\frac{C^2}{2\theta} - \frac{3}{2} \right) \frac{1}{\theta} \frac{\partial \theta}{\partial x_u} + \frac{C_i}{\theta} \frac{\partial v_i}{\partial x_u} \right]. \quad (5.8)$$

The term $(\partial \hat{f}_M / \partial x_u) \Phi$ is nonlinear in the non-equilibrium moments and gradients of temperature and velocity, hence will be dropped in linearization. Within the linearization, the derivative of Φ is simply the same expression for Φ as in (3.5), except that the moments $\Delta, \sigma_{ij}, q_i, R_{ij}, m_{ijk}$ are replaced by their gradients.

Explicitly, we find for the first derivative (semi-linearized)

$$\frac{\partial f_{|26}}{\partial x_u} = \hat{f}_M \left[\begin{aligned} & \frac{\partial \rho}{\partial x_u} + \frac{\rho}{\theta} \frac{\partial v_i}{\partial x_u} C_i + \frac{\rho}{\theta} \frac{\partial \theta}{\partial x_u} \left(\frac{C^2}{2\theta} - \frac{3}{2} \right) \\ & + \frac{1}{8\theta^2} \frac{\partial \Delta}{\partial x_u} \left(1 - \frac{2}{3} \frac{C^2}{\theta} + \frac{1}{15} \frac{C^4}{\theta^2} \right) \\ & + \frac{2}{5} \frac{1}{\theta^2} \frac{\partial q_k}{\partial x_u} C_k \left(\frac{C^2}{2\theta} - \frac{5}{2} \right) + \frac{1}{2\theta^2} \frac{\partial \sigma_{ij}}{\partial x_u} C_{(i} C_{j)} \\ & + \frac{1}{14\theta^3} \frac{\partial R_{ij}}{\partial x_u} C_{(i} C_{j)} \left(\frac{C^2}{2\theta} - \frac{7}{2} \right) + \frac{1}{6\theta^3} \frac{\partial m_{ijk}}{\partial x_u} C_{(i} C_{j} C_{k)} \end{aligned} \right]. \quad (5.9)$$

Generalization to higher derivatives yields (we require this for $n = 1, 2, 3$)

$$\frac{\partial^n f_{26}}{\partial x_{u_1} \cdots \partial x_{u_n}} = \hat{f}_M \left[\begin{aligned} & \frac{\partial^n \rho}{\partial x_{u_1} \cdots \partial x_{u_n}} + \mathcal{A}_{[u_1 \cdots u_n]i} \frac{C_i}{\theta} + \frac{1}{\theta} \mathcal{B}_{[u_1 \cdots u_n]} \left(\frac{C^2}{2\theta} - \frac{3}{2} \right) \\ & + \frac{1}{8\theta^2} \frac{\partial^n \Delta}{\partial x_{u_1} \cdots \partial x_{u_n}} \left(1 - \frac{2}{3} \frac{C^2}{\theta} + \frac{1}{15} \frac{C^4}{\theta^2} \right) \\ & + \frac{2}{5} \frac{1}{\theta^2} \frac{\partial^n q_k}{\partial x_{u_1} \cdots \partial x_{u_n}} C_k \left(\frac{C^2}{2\theta} - \frac{5}{2} \right) + \frac{1}{2\theta^2} \frac{\partial^n \sigma_{ij}}{\partial x_{u_1} \cdots \partial x_{u_n}} C_{(i} C_{j)} \\ & + \frac{1}{14\theta^3} \frac{\partial^n R_{ij}}{\partial x_u \partial x_v \partial x_w} C_{(i} C_{j)} \left(\frac{C^2}{2\theta} - \frac{7}{2} \right) + \frac{1}{6\theta^3} \frac{\partial^n m_{ijk}}{\partial x_{u_1} \cdots \partial x_{u_n}} C_{(i} C_{j} C_{k)} \end{aligned} \right] \quad (5.10)$$

where

$$\left. \begin{aligned} \mathcal{A}_{[u]i} &= \left(\frac{\partial \rho v_i}{\partial x_u} - v_i \frac{\partial \rho}{\partial x_u} \right) = \left(\rho \frac{\partial v_i}{\partial x_u} \right), \\ \mathcal{A}_{[uv]i} &= \left(\frac{\partial^2 \rho v_i}{\partial x_u \partial x_v} - v_i \frac{\partial^2 \rho}{\partial x_u \partial x_v} \right), \\ \mathcal{A}_{[uvw]i} &= \left(\frac{\partial^3 \rho v_i}{\partial x_u \partial x_v \partial x_w} - v_i \frac{\partial^3 \rho}{\partial x_u \partial x_v \partial x_w} \right), \end{aligned} \right\} \quad (5.11)$$

and

$$\left. \begin{aligned} \mathcal{B}_{[u]} &= \left(\frac{\partial \rho \theta}{\partial x_u} - \theta \frac{\partial \rho}{\partial x_u} \right) = \left(\rho \frac{\partial \theta}{\partial x_u} \right), \\ \mathcal{B}_{[uv]} &= \left(\frac{\partial^2 \rho \theta}{\partial x_u \partial x_v} - \theta \frac{\partial^2 \rho}{\partial x_u \partial x_v} \right), \\ \mathcal{B}_{[uvw]} &= \left(\frac{\partial^3 \rho \theta}{\partial x_u \partial x_v \partial x_w} - \theta \frac{\partial^3 \rho}{\partial x_u \partial x_v \partial x_w} \right). \end{aligned} \right\} \quad (5.12)$$

Here, square brackets around indices are just a notational convenience, used for identification of different index groups.

5.4. Expansion of the production terms

We now insert the above expansions into the expression (5.3) for the moment productions, and consider contributions up to fifth-order terms in particle diameter a . We sort by order

in a , to write the moment production (where f stands for $f_{[26]}$) as

$$\begin{aligned}
 \mathcal{P}_\psi &= a^2 Y \int \int f^1 f \left[g \int_0^{2\pi} \int_0^{\pi/2} (\psi' - \psi) \cos \theta \sin \theta \, d\theta \, d\varepsilon \right] \mathbf{dc}^1 \, \mathbf{dc} \\
 &- a^3 \int \int \left(Y_{ri} f^1 f + Y \frac{\partial f^1}{\partial x_r} f \right) \left[g \int_0^{2\pi} \int_0^{\pi/2} (\psi' - \psi) k_r \cos \theta \sin \theta \, d\theta \, d\varepsilon \right] \mathbf{dc}^1 \, \mathbf{dc} \\
 &+ a^4 \int \int \left(Y_{rs} f^1 f + Y_r \frac{\partial f^1}{\partial x_s} f + \frac{1}{2} Y \frac{\partial^2 f^1}{\partial x_r \partial x_s} f \right) \\
 &\times \left[g \int_0^{2\pi} \int_0^{\pi/2} (\psi' - \psi) k_r k_s \cos \theta \sin \theta \, d\theta \, d\varepsilon \right] \mathbf{dc}^1 \, \mathbf{dc} \\
 &- a^5 \int \int \left(\begin{aligned} &Y_{rst} f^1 f + Y_{rs} \frac{\partial f^1}{\partial x_t} f \\ &+ \frac{1}{2} Y_r \frac{\partial^2 f^1}{\partial x_s \partial x_t} f + \frac{1}{6} Y \frac{\partial^3 f^1}{\partial x_r \partial x_s \partial x_t} f \end{aligned} \right) \\
 &\times \left[g \int_0^{2\pi} \int_0^{\pi/2} (\psi' - \psi) k_r k_s k_t \cos \theta \sin \theta \, d\theta \, d\varepsilon \right] \mathbf{dc}^1 \, \mathbf{dc}. \tag{5.13}
 \end{aligned}$$

There will be further linearization in the terms quadratic in the distribution functions and their derivatives, where we will ignore nonlinear terms in non-equilibrium contributions. The first line above is the standard production for hard-sphere molecules; the others are correction terms from the Enskog term.

The Vlasov force has fifth-order terms that remain in equilibrium, and are required for the computation of the interface. For our first approach to moment equations for EV, in our linearization of \mathcal{P}_ψ we will consider only those fifth-order terms that remain in equilibrium, while non-equilibrium contributions will be considered only up to fourth order in a .

The evaluation of these integrals is rather involved, and it is impossible to discuss all the details. In the following sections, we outline the main steps for the computation of the \mathcal{P}_ψ .

5.5. Velocity transformation

Computation of the production integrals is a standard procedure in kinetic theory; here, it is just more involved, due to the larger number of contributions to the productions. Solution of all integrals implies change of variables from C , C^1 to

$$g_i = C_i^1 - C_i, \quad G_i = \frac{1}{2}(C_i + C_i^1), \tag{5.14a,b}$$

or the inverse,

$$C_i = G_i - \frac{1}{2}g_i, \quad C_i^1 = G_i + \frac{1}{2}g_i. \tag{5.15a,b}$$

Use of the peculiar velocity implies that we look at the collision terms from the rest frame of the gas, which is natural when we use central moments.

We also have

$$C^2 = G^2 - G_i g_i + \frac{g^2}{4}, \quad (C^1)^2 = G^2 + G_i g_i + \frac{g^2}{4}, \quad C^2 + (C^1)^2 = 2G^2 + \frac{g^2}{2} \tag{5.16a-c}$$

and

$$dc dc^1 = dC dC^1 = \left\| \frac{\partial(C, C^1)}{\partial(G, g)} \right\| dG dg = \begin{vmatrix} \delta_{ij} & -\frac{1}{2}\delta_{ij} \\ \delta_{ij} & +\frac{1}{2}\delta_{ij} \end{vmatrix} dG dg = dG dg. \tag{5.17}$$

5.6. *k*-integration

We have $\psi(C_k) = mC_{i_1} \cdots C_{i_n}$ and $C'_i = C_i + k_i g \cos \theta$. In (5.13), the direction vector k_i appears only in ψ' and in the integrals in square brackets, but not in the distribution function terms. Therefore, we can deal with the k -integrals first.

The explicit dependence of ψ on k is as follows. For $\psi(C_k) = m$,

$$\frac{1}{m} (\psi' - \psi) = 0; \tag{5.18}$$

for $\psi(C_k) = mC_i$,

$$\frac{1}{m} (\psi' - \psi) = g \cos \theta k_i; \tag{5.19}$$

for $\psi(C_k) = mC_i C_j$,

$$\frac{1}{m} (\psi' - \psi) = 2C_{(i} k_j) g \cos \theta + k_i k_j g^2 \cos^2 \theta; \tag{5.20}$$

for $\psi(C_k) = mC_i C_j C_k$,

$$\frac{1}{m} (\psi' - \psi) = 3C_{(i} C_j k_k) g \cos \theta + 3C_{(i} k_j k_k) g^2 \cos^2 \theta + k_i k_j k_k g^3 \cos^3 \theta; \tag{5.21}$$

for $\psi(C_k) = mC^2 C_i C_j$,

$$\begin{aligned} \frac{1}{m} (\psi' - \psi) &= 2C_i C_j C_k k_k g \cos \theta + 2C^2 C_{(i} k_j) g \cos \theta + C_i C_j g^2 \cos^2 \theta \\ &+ 4C_k C_{(i} k_j) k_k g^2 \cos^2 \theta + C^2 k_i k_j g^2 \cos^2 \theta + 2C_{(i} k_j) g^3 \cos^3 \theta \\ &+ 2C_k k_i k_j k_k g^3 \cos^3 \theta + k_i k_j g^4 \cos^4 \theta. \end{aligned} \tag{5.22}$$

Insertion of the above into the production terms shows that we are facing integrals, for $n \leq 3$ and $m \leq 3$, of the type

$$[I_{m,n}^\alpha]_{i_1 \dots i_{n+m}} = g^{n+\alpha+1} \int_0^{2\pi} \int_0^{\pi/2} k_{i_1} \dots k_{i_{n+m}} \cos^{n+\alpha+1} \theta \sin \theta \, d\theta \, d\varepsilon, \quad (5.23)$$

where $k_k = \{\cos \varepsilon \sin \theta, \sin \varepsilon \sin \theta, \cos \theta\}_k$ and $k_k g_k = g \cos \theta$. Explicit expressions for the integrals required are given in [Appendix A](#).

5.7. Explicit productions

The next step is to insert the integrals $[I_{m,n}^\alpha]_{i_1 \dots i_{n+m}}$ into (5.13), which gives explicit integrals of $f^1 f$ and $(\partial^n f_{|26}^1 / \partial x_{u_1} \dots \partial x_{u_n}) f$ over polynomials in g_i and C_i ; for these integrations, C_i must be expressed through g_i and G_i . These integrals were evaluated on the computer, using Wolfram Mathematica™. Results are inserted and simplified to produce the final expressions for the production terms.

5.7.1. Density, $\psi(C_k) = m$

As we have seen already, there is no contribution to mass balance:

$$\mathcal{P}_m = \mathcal{P}^0 = 0. \quad (5.24)$$

5.7.2. Momentum, $\psi(C_k) = mC_i$

The production terms for momentum and energy do not vanish, since in the collision momentum and energy are transferred across the diameter, a , that is, the distance between the centres of mass of the colliding hard spheres. However, for collision invariants, non-local production terms can be recast in divergence form (Karkheck & Stell 1981). This property is inherited by the local expansion at any order, of course.

We take a closer look at the computation of the momentum production term, but for the other productions we will just present the results. After insertion of the integrals $[I_{m,n}^\alpha]_{i_1 \dots i_{n+m}}$, the momentum production term reads

$$\begin{aligned} \mathcal{P}_{mC_i} = \mathcal{P}_i^0 &= \frac{\pi}{2} m a^2 Y \iint f^1 f \{g_i g_i\} \, d\mathbf{G} \, d\mathbf{g} \\ &- \frac{2\pi}{15} m a^3 \iint \left(Y_r f^1 f + Y \frac{\partial f^1}{\partial x_r} f \right) \left\{ g^2 \delta_{ir} + 2g_i g_r \right\} \, d\mathbf{G} \, d\mathbf{g} \\ &+ \frac{\pi}{12} m a^4 \iint \left(Y_{rs} f^1 f + Y_r \frac{\partial f^1}{\partial x_s} f + \frac{1}{2} Y \frac{\partial^2 f^1}{\partial x_r \partial x_s} f \right) \left\{ 3g \delta_{(ir} g_s) + \frac{g_i g_r g_s}{g} \right\} \, d\mathbf{G} \, d\mathbf{g} \\ &- \frac{2\pi}{35} m a^5 \iint \left(\begin{array}{c} Y_{rst} f^1 f + Y_{rs} \frac{\partial f^1}{\partial x_t} f \\ + \frac{1}{2} Y_r \frac{\partial^2 f^1}{\partial x_s \partial x_t} f + \frac{1}{6} Y \frac{\partial^3 f^1}{\partial x_r \partial x_s \partial x_t} f \end{array} \right) \\ &\times \left\{ g^2 \delta_{(ir} \delta_{st}) + 4\delta_{(ir} g_s g_t) \right\} \, d\mathbf{G} \, d\mathbf{g}. \end{aligned} \quad (5.25)$$

Obviously, there is a larger number of integrals over $f^1 f$ and $(\partial^n f^1 / \partial x^n) f$ that must be determined and inserted; see [Appendix B](#) for a brief discussion and some results.

Inserting the integrals, and making use of (5.5a–d), we finally find the momentum collision term, as expected in divergence form:

$$\mathcal{P}_{mC_i} = -\frac{\partial}{\partial x_r} \left\{ \begin{array}{l} \left[\frac{2\pi}{3} \frac{\rho a^3}{m} Y \left(\rho\theta\delta_{ir} + \frac{2}{5}\sigma_{ir} \right) \right] \\ - \left[\frac{2\pi}{3} \frac{a^4}{m\sqrt{\pi\theta}} \rho^2 Y \frac{6}{5} \left(\theta \frac{\partial\delta_{(ir)v_s}}{\partial x_s} + \frac{1}{10} \frac{\partial\delta_{(ir)q_s}}{\partial x_s} + \frac{1}{42} \frac{\partial m_{irs}}{\partial x_s} \right) \right] \\ + \left[\frac{\pi}{60} \frac{a^5}{m} \left(\frac{\partial^2 Y \rho^2 \theta}{\partial x_s \partial x_t} + 3Y \frac{\partial^2 \rho^2 \theta}{\partial x_s \partial x_t} - 12Y \frac{\partial \rho}{\partial x_s} \frac{\partial \rho \theta}{\partial x_t} \right) \delta_{(ir)\delta_{st}} \right] \end{array} \right\}. \quad (5.26)$$

We emphasize that to reach the above, we have ignored nonlinear terms between non-equilibrium contributions. Moreover, as stated before, we have kept only those fifth-order terms that contribute in equilibrium, where the density gradient is non-zero in the interface, while we removed fifth-order terms that contribute only in non-equilibrium, assuming that their influence is decidedly smaller.

5.7.3. 2-tensor, $\psi(C_k) = mC_i C_j$

The Enskog contribution to energy is half of the trace, $\psi(C_k) = \frac{1}{2}mC^2$, and the contribution to the stress tensor is the trace-free part, $\psi(C_k) = mC_{(i}C_{j)}$; we list both contributions separately. Moreover, for more transparent presentation of the results, we show contributions of different orders in the expansion.

Order a^2

The leading terms correspond to results from the Boltzmann collision term for hard spheres, except that the correlation function Y appears as a correction factor. There is no contribution to energy, only to stress:

$$\mathcal{P}_{(1/2)mC^2}^{(2)} = 0, \quad (5.27)$$

$$\mathcal{P}_{mC_{(i}C_{j)}}^{(2)} = -\frac{16}{5} \frac{\rho\sqrt{\pi\theta}a^2}{m} Y \left(\sigma_{ij} + \frac{1}{28} \frac{R_{ij}}{\theta} \right). \quad (5.28)$$

With the relaxation time τ defined through

$$\frac{1}{\tau} = \frac{16}{5} \frac{\rho\sqrt{\pi\theta}a^2}{m} Y, \quad (5.29)$$

we can write the last expression as $\mathcal{P}_{mC_{(i}C_{j)}}^{(2)} = -(1/\tau) \left(\sigma_{ij} + \frac{1}{28} (R_{ij}/\theta) \right)$. The same relaxation time will appear in other second-order expressions below.

Order a^3

To third order, there is a contribution to thermal energy, which is related to energy transfer over the distance a of the colliding particles:

$$P_{(1/2)mC^2}^{(3)} = -\frac{2\pi}{3} \frac{a^3}{m} \left\{ \rho^2 \theta Y \frac{\partial v_r}{\partial x_r} + \frac{3}{5} \frac{\partial \rho Y q_r}{\partial x_r} \right\}, \quad (5.30)$$

$$P_{mC_{(i)C_{(j)}}}^{(3)} = -\frac{2\pi}{3} \frac{a^3}{m} \left\{ \begin{aligned} &\frac{4}{5} \rho^2 \theta Y \frac{\partial v_{(i)}}{\partial x_{(j)}} + \frac{12}{25} \frac{\partial \rho Y q_{(i)}}{\partial x_{(j)}} + \frac{6}{25} \frac{q_{(i)}}{\rho} \frac{\partial \rho^2 Y}{\partial x_{(j)}} \\ &+ \frac{6}{35} \frac{\partial \rho Y m_{ijr}}{\partial x_r} + \frac{8}{35} \frac{m_{ijr}}{\rho} \frac{\partial \rho^2 Y}{\partial x_r} \end{aligned} \right\}. \quad (5.31)$$

The contribution to total energy results from adding the corresponding term for kinetic energy; see (4.11). Within the linearizations performed, the contribution to total energy can be written in divergence form as

$$\mathcal{P}_{(1/2)mC^2}^{(3)} + v_i \mathcal{P}_{mC_i}^{(3)} = -\frac{\partial}{\partial x_r} \left\{ \frac{2\pi}{3} \frac{a^3}{m} \rho Y \left[\rho \theta v_r + \frac{3}{5} q_r + \frac{2}{5} v_i \sigma_{ir} \right] \right\}. \quad (5.32)$$

This form is shown to give evidence that the Enskog collision term leads not to an actual energy production, but rather to energy transfer, as described by the flux under the divergence.

Order a^4

The contributions to energy and stress equations to fourth order read

$$\begin{aligned} &\mathcal{P}_{(1/2)mC^2}^{(4)} \\ &= \frac{\partial}{\partial x_r} \left\{ \frac{2\pi}{15} \frac{a^4}{m\sqrt{\pi}} \rho^2 Y \left[5\sqrt{\theta} \frac{\partial \theta}{\partial x_r} + \frac{1}{12} \frac{1}{\sqrt{\theta}} \frac{\partial}{\partial x_r} \left(\frac{\Delta}{\rho} \right) + 2\sqrt{\theta} \frac{\partial}{\partial x_s} \left(\frac{\sigma_{rs}}{\rho} \right) + \frac{1}{7} \frac{1}{\sqrt{\theta}} \frac{\partial}{\partial x_s} \left(\frac{R_{rs}}{\rho} \right) \right] \right\}, \end{aligned} \quad (5.33)$$

$$\begin{aligned} &\mathcal{P}_{mC_{(i)C_{(j)}}}^{(4)} = \frac{4}{105} \frac{\sqrt{\pi} a^4}{m} \frac{1}{\sqrt{\theta}} \\ &\left(\begin{aligned} &14\theta \frac{\partial}{\partial x_{(i)}} \left(\rho^2 Y \frac{\partial \theta}{\partial x_{(j)}} \right) + \frac{7}{30} \frac{\partial}{\partial x_{(i)}} \left(\rho^2 Y \frac{\partial}{\partial x_{(j)}} \left(\frac{\Delta}{\rho} \right) \right) \\ &+ 2\theta \rho \frac{\partial}{\partial x_r} \left(Y \frac{\partial \sigma_{ij}}{\partial x_r} \right) - 12\theta \sigma_{ij} \frac{\partial}{\partial x_r} \left(Y \frac{\partial \rho}{\partial x_r} \right) - \frac{5}{2} \rho \theta \sigma_{ij} \frac{\partial^2 Y}{\partial x_r \partial x_r} \\ &+ 8\theta \rho \frac{\partial}{\partial x_{(r)}} \left(Y \frac{\partial \sigma_{r(i)\delta_{j)s}}}{\partial x_s} \right) - 20\theta \sigma_{r(i)\delta_{j)s}} \frac{\partial}{\partial x_{(r)}} \left(Y \frac{\partial \rho}{\partial x_s} \right) \\ &\qquad\qquad\qquad - 3\rho \theta \sigma_{r(i)\delta_{j)s}} \frac{\partial^2 Y}{\partial x_r \partial x_s} \\ &+ \frac{1}{7} \rho \frac{\partial}{\partial x_r} \left(Y \frac{\partial R_{ij}}{\partial x_r} \right) - \frac{1}{2} R_{ij} \frac{\partial}{\partial x_r} \left(Y \frac{\partial \rho}{\partial x_r} \right) - \frac{5}{56} \rho R_{ij} \frac{\partial^2 Y}{\partial x_r \partial x_r} \\ &+ \frac{4}{7} \rho \frac{\partial}{\partial x_{(r)}} \left(Y \frac{\partial R_{r(i)\delta_{j)s}}}{\partial x_s} \right) - R_{r(i)\delta_{j)s}} \frac{\partial}{\partial x_{(r)}} \left(Y \frac{\partial \rho}{\partial x_s} \right) \\ &\qquad\qquad\qquad - \frac{3}{28} \rho R_{r(i)\delta_{j)s}} \frac{\partial^2 Y}{\partial x_r \partial x_s} \end{aligned} \right). \end{aligned} \quad (5.34)$$

Within the linearizations performed, we find the fourth-order contribution to energy as $\mathcal{P}_{(1/2)mC^2}^{(4)} + v_i \mathcal{P}_{mC_i}^{(4)} \simeq \mathcal{P}_{(1/2)mC^2}^{(4)}$, which is of divergence form. Obviously, the linearization removed terms that bring the full expression to divergence form.

All fifth-order terms vanish in equilibrium, and are ignored.

5.7.4. 3-tensor, $\psi(C_k) = mC_i C_j C_k$

For the Enskog contribution to energy flux, we need half of the trace, $\psi(C_k) = \frac{1}{2}mC^2 C_i$, and for the contribution to the third moment we need the trace-free part, $\psi(C_k) = mC_{(i} C_j C_{k)}$; we list both contributions separately. The overall contribution to the heat flux equation (3.11) is the combination

$$\mathcal{P}_i^{HF} = \frac{1}{2} \mathcal{P}_i^1 - \frac{5}{2} \theta \mathcal{P}_i^0 - \frac{\sigma_{ik}}{\rho} \mathcal{P}_k^0 = \mathcal{P}_{(1/2)mC^2 C_i} - \frac{5}{2} \theta \mathcal{P}_{mC_i} - \frac{\sigma_{ik}}{\rho} \mathcal{P}_{mC_k}, \quad (5.35)$$

and for the contribution to the equations for m_{ijk} we need the combination $\mathcal{P}_{ijk}^0 - 3\sigma_{(ij} / \rho \mathcal{P}_{k)}$. These will be given as well.

Again, for more transparent presentation of the results, we show contributions of different orders in the expansion.

Order a^2

The leading terms correspond to results from the Boltzmann collision term for hard spheres, except that the correlation Y function appears as a correction factor:

$$\mathcal{P}_{(1/2)mC^2 C_i}^{(2)} = -\frac{2}{3} \frac{16}{5} \frac{\rho \sqrt{\pi \theta} a^2}{m} Y q_i, \quad (5.36)$$

$$\mathcal{P}_{mC_{(i} C_j C_{k)}}^{(2)} = -\frac{3}{2} \frac{16}{5} \frac{\rho \sqrt{\pi \theta} a^2}{m} Y m_{ijk}. \quad (5.37)$$

With the relaxation time τ introduced for the stress contribution, we can write these as $\mathcal{P}_{(1/2)mC^2 C_i}^{(2)} = -\frac{2}{3}(q_i/\tau)$ and $\mathcal{P}_{mC_{(i} C_j C_{k)}}^{(2)} = -\frac{3}{2}(1/\tau)m_{ijk}$; these have the same factors $\frac{2}{3}$ and $\frac{3}{2}$ that one finds for hard spheres and Maxwell molecules; see Gupta & Torrillon (2012).

Order a^3

We find

$$\mathcal{P}_{(1/2)mC^2 C_i}^{(3)} = -\frac{2\pi}{3} \frac{a^3}{m} \left\{ \begin{aligned} &4\theta \frac{\partial Y \rho^2 \theta}{\partial x_k} - \frac{3}{2} \theta^2 \frac{\partial \rho^2 Y}{\partial x_k} + \frac{1}{10} \frac{\partial \rho Y \Delta}{\partial x_k} + \frac{1}{30} \frac{\Delta}{\rho} \frac{\partial \rho^2 Y}{\partial x_k} \\ &+ \frac{8}{5} \frac{\partial \rho Y \theta \sigma_{kr}}{\partial x_r} + \frac{1}{10} \frac{\theta \sigma_{kr}}{\rho} \frac{\partial \rho^2 Y}{\partial x_r} + \frac{6}{35} \frac{\partial \rho Y R_{kr}}{\partial x_r} + \frac{11}{140} \frac{R_{kr}}{\rho} \frac{\partial \rho^2 Y}{\partial x_r} \end{aligned} \right\}, \quad (5.38)$$

$$\mathcal{P}_{mC_{(i} C_j C_{k)}}^{(3)} = -\frac{2\pi}{3} \frac{a^3}{m} \left[\begin{aligned} &\frac{18}{35} \frac{\partial \rho Y \theta \sigma_{(ij}}{\partial x_k)} + \frac{9}{5} \frac{\theta \sigma_{(ij}}{\rho} \frac{\partial \rho^2 Y}{\partial x_k)} \\ &+ \frac{36}{245} \frac{\partial \rho Y R_{(ij}}{\partial x_k)} + \frac{93}{490} \frac{R_{(ij}}{\rho} \frac{\partial \rho^2 Y}{\partial x_k)} \end{aligned} \right]. \quad (5.39)$$

The corresponding production term in the heat flux equation (3.11) reads, after appropriate linearization,

$$\mathcal{P}_i^{HF(3)} = -\frac{2\pi}{3} \frac{a^3}{m} \left[\begin{aligned} & \frac{3}{2} \rho^2 Y \theta \frac{\partial \theta}{\partial x_i} + \frac{1}{10} \frac{\partial \rho Y \Delta}{\partial x_i} + \frac{1}{30} \frac{\Delta}{\rho} \frac{\partial \rho^2 Y}{\partial x_i} \\ & + \frac{3}{5} \frac{\partial \rho Y \theta \sigma_{ir}}{\partial x_r} - \frac{9}{10} \frac{\sigma_{ik}}{\rho} \frac{\partial \rho^2 \theta Y}{\partial x_k} \\ & + \frac{6}{35} \frac{\partial \rho Y R_{ir}}{\partial x_r} + \frac{11}{140} \frac{R_{ir}}{\rho} \frac{\partial \rho^2 Y}{\partial x_r} \end{aligned} \right]. \quad (5.40)$$

The contribution for the m_{ijk} equation (3.14) becomes

$$\mathcal{P}_{ijk}^0 - \frac{3\sigma_{(ij}}{\rho} \mathcal{P}_k^0 = -\frac{2\pi}{3} \frac{a^3}{m} \left[\begin{aligned} & \frac{18}{35} \theta \frac{\partial \rho Y \sigma_{(ij}}{\partial x_k)} - \frac{6}{5} \frac{\theta \sigma_{(ij}}{\rho} \frac{\partial \rho^2 Y}{\partial x_k)} + \frac{36}{245} \frac{\partial \rho Y R_{(ij}}{\partial x_k)} \\ & + \frac{93}{490} \frac{R_{(ij}}{\rho} \frac{\partial \rho^2 Y}{\partial x_k)} \end{aligned} \right]. \quad (5.41)$$

Order a^4

For the fourth-order contribution to heat flux, we find the full production as

$$\mathcal{P}_k^{HF(4)} = \frac{\sqrt{\pi} a^4}{m} \sqrt{\theta} \left[\begin{aligned} & -\frac{19}{15} \theta \left[\frac{\partial}{\partial x_r} \left(\rho^2 Y \frac{\partial v_k}{\partial x_r} \right) + 2 \frac{\partial}{\partial x_{(k}} \left(\rho^2 Y \frac{\partial v_r}{\partial x_r} \right) \right] \\ & - \frac{53}{70} \rho \frac{\partial}{\partial x_r} \left(Y \frac{\partial q_k}{\partial x_r} \right) - \frac{1}{2} q_k \frac{\partial}{\partial x_r} \left(Y \frac{\partial \rho}{\partial x_r} \right) - \frac{2}{25} \rho q_k \frac{\partial^2 Y}{\partial x_r \partial x_r} \\ & - \frac{7}{15} q_r \frac{\partial}{\partial x_{(k}} \left(Y \frac{\partial \rho}{\partial x_r} \right) + \frac{169}{105} \rho \frac{\partial}{\partial x_{(k}} \left(Y \frac{\partial q_r}{\partial x_r} \right) - \frac{2}{75} \rho q_r \frac{\partial^2 Y}{\partial x_r \partial x_k} \\ & + \frac{9}{70} \rho \frac{\partial}{\partial x_r} \left(Y \frac{\partial m_{krs}}{\partial x_s} \right) - \frac{1}{6} m_{irs} \frac{\partial}{\partial x_r} \left(Y \frac{\partial \rho}{\partial x_s} \right) - \rho \frac{1}{105} m_{krs} \frac{\partial^2 Y}{\partial x_r \partial x_s} \end{aligned} \right]. \quad (5.42)$$

The total contribution to the fourth-order terms for the m_{ijk} equation (3.14) reads

$$\mathcal{P}_{m_{ijk}} = \frac{\sqrt{\pi} a^4}{m} \sqrt{\theta} \left[\begin{aligned} & \frac{4}{35} \theta \frac{\partial}{\partial x_{(i}} \left(\rho^2 Y \frac{\partial v_j}{\partial x_k)} \right) \\ & - \frac{22}{35} \rho \frac{\partial}{\partial x_{(i}} \left(Y \frac{\partial q_j}{\partial x_k)} \right) - \frac{2}{5} q^{(i} \frac{\partial}{\partial x_j} \left(Y \frac{\partial \rho}{\partial x_k)} \right) - \frac{4}{175} \rho q^{(i} \frac{\partial^2 Y}{\partial x_j \partial x_k)} \\ & + \frac{2}{70} \rho \frac{\partial}{\partial x_r} \left(Y \frac{\partial m_{ijk}}{\partial x_r} \right) - \frac{3}{5} m_{ijk} \frac{\partial}{\partial x_r} \left(Y \frac{\partial \rho}{\partial x_r} \right) - \frac{1}{7} \rho m_{ijk} \frac{\partial^2 Y}{\partial x_r \partial x_r} \\ & + \frac{6}{70} \rho \frac{\partial}{\partial x_r} \left(Y \frac{\partial m_{r(ij}}{\partial x_k)} \right) + \frac{6}{70} \rho \frac{\partial}{\partial x_{(i}} \left(Y \frac{\partial m_{j)kr}}{\partial x_r} \right) - \frac{3}{7} m_{r(ij} \frac{\partial}{\partial x_k)} \left(Y \frac{\partial \rho}{\partial x_r} \right) \\ & - \frac{3}{7} m_{r(ij} \frac{\partial}{\partial x_r} \left(Y \frac{\partial \rho}{\partial x_k)} \right) - \frac{6}{35} \rho m_{r(ij} \frac{\partial^2 Y}{\partial x_k) \partial x_r} \end{aligned} \right]. \quad (5.43)$$

5.7.5. Trace of 4-tensor, $\psi(C_k) = mC^2 C_i C_j$

Again, we distinguish the trace and trace-free parts, at different orders. These are the contributions to equations (3.10) and (3.13) for higher moments Δ and R_{ij} .

Order a^2

The leading terms correspond to results from the Boltzmann collision term for hard spheres, except that the correlation function appears as a correction factor:

$$\mathcal{P}_{mC^4}^{(2)} = -\frac{2}{3} \frac{16}{5} \frac{a^2 \rho \sqrt{\pi \theta}}{m} Y \Delta, \tag{5.44}$$

$$\mathcal{P}_{mC^2 C_{(i} C_{j)}}^{(2)} = -\frac{16}{5} \frac{a^2 \rho \sqrt{\pi \theta}}{m} Y \left[\frac{15}{2} \theta \sigma_{ij} + \frac{247}{168} R_{ij} \right]. \tag{5.45}$$

Once more, we find the hard-sphere relaxation time $1/\tau = \frac{16}{5} (\rho \sqrt{\pi \theta} a^2 / m) Y$. The coefficients $(\frac{2}{3}, \frac{15}{2}, \frac{247}{168})$ agree with the results for hard spheres by Gupta & Torrilhon (2012).

Order a^3

The third-order contributions are

$$\mathcal{P}_{mC^4}^{(3)} = -\frac{2}{3} \frac{\pi \theta a^3}{m} \left\{ \frac{84}{5} \frac{\partial Y \rho q_r}{\partial x_r} + \frac{8}{5} \frac{q_r}{\rho} \frac{\partial Y \rho^2}{\partial x_r} + 20 Y \theta \rho^2 \frac{\partial v_r}{\partial x_r} \right\}, \tag{5.46}$$

$$\mathcal{P}_{mC^2 C_{(i} C_{j)}}^{(3)} = -\frac{2\pi}{3} \frac{a^3}{m} \theta \left\{ \begin{aligned} &\frac{132}{25} \frac{\partial \rho Y q_{(i}}{\partial x_{j)}} + \frac{112}{25} \frac{q_{(i}}{\rho} \frac{\partial \rho^2 Y}{\partial x_{j)}} + \frac{28}{5} Y \theta \rho^2 \frac{\partial v_{(i}}{\partial x_{j)}} \\ &+ \frac{66}{35} \frac{\partial Y \rho m_{ijr}}{\partial x_r} + \frac{71}{35} \frac{m_{ijr}}{\rho} \frac{\partial Y \rho^2}{\partial x_r} \end{aligned} \right\}. \tag{5.47}$$

For the balance laws (3.10), (3.13) for Δ and R_{ij} , we find the required combinations up to third order, after linearization:

$$\begin{aligned} \mathcal{P}^2 - 20\theta \frac{\mathcal{P}^1}{2} - \frac{8q_k}{\rho} \mathcal{P}_k^0 &= -\frac{2}{3} \left[\frac{16}{5} \frac{a^2 \rho \sqrt{\pi \theta}}{m} Y \right] \Delta \\ &\quad - \frac{2\pi}{3} \frac{a^3}{m} \theta \left[\frac{24}{5} \frac{\partial \rho Y q_r}{\partial x_r} - \frac{32}{5} \frac{q_k}{\rho} \frac{\partial Y \rho^2}{\partial x_k} \right], \end{aligned} \tag{5.48}$$

$$\begin{aligned} \mathcal{P}_{ij}^1 - 7\theta \mathcal{P}_{ij}^0 - \frac{14}{3} \frac{\sigma_{ij}}{\rho} \frac{\mathcal{P}^1}{2} - 2 \frac{m_{ijk}}{\rho} \mathcal{P}_k^0 - \frac{28}{5} \frac{q_{(i}}{\rho} \mathcal{P}_{j)}^0 \\ = -\frac{16}{5} \frac{a^2 \rho \sqrt{\pi \theta}}{m} Y \left[\frac{1}{2} \theta \sigma_{ij} + \frac{205}{168} R_{ij} \right] - \frac{2\pi}{3} \frac{a^3}{m} \theta \left[\frac{48}{25} \frac{\partial \rho Y q_{(i}}{\partial x_{j)}} \right. \\ \left. - \frac{14}{5} \frac{q_{(i}}{\rho} \frac{\partial \rho^2 Y}{\partial x_{j)}} + \frac{24}{35} \frac{\partial \rho Y m_{ijr}}{\partial x_r} - \frac{11}{7} \frac{m_{ijk}}{\rho} \frac{\partial \rho^2 Y}{\partial x_k} \right]. \end{aligned} \tag{5.49}$$

The fourth-order contributions are not shown separately, but are included in the full equations shown below.

6. Linearized transport equations up to fourth order

Next, we combine the above results, that is, we insert all Enskog and Vlasov terms into the transport equations, and simplify as much as possible.

We remind the reader that the equations were derived based on several simplifying approximations, as follows.

- (a) All equations are linearized for small deviations from equilibrium. Nonlinear terms involving density gradients were retained, since equilibrium states for phase equilibrium include density gradients in the interface.
- (b) Non-localities in the Enskog collision term were replaced with gradient terms by means of Taylor expansions with the particle diameter a as the relevant smallness parameter. To include equilibrium capillary pressures properly, terms of fifth order are included in the balance of momentum. Indeed, the balance of momentum is the only equation in which fifth-order equilibrium terms appear, while in the other equations, terms of fifth order appear only as non-equilibrium contributions. For this first approach to moment equations for EV, we considered non-equilibrium contributions only to fourth order in a .

The complete equations are presented with some comments in the sections below.

6.1. Mass balance

The mass balance is not affected by the Enskog collision term; it has the usual form,

$$\frac{\partial \rho}{\partial t} + \frac{\partial \rho v_k}{\partial x_k} = 0. \tag{6.1}$$

6.2. Momentum balance

The momentum balance is best written in conservative form, with the total momentum flux in the divergence. For order a^5 , we consider only equilibrium contributions:

$$\rho \frac{Dv_i}{Dt} + \frac{\partial}{\partial x_k} \left(\begin{aligned} & \left[\rho \theta \left(1 + \frac{2\pi}{3} \frac{a^3}{m} \rho Y \right) - \frac{2\pi a^3}{3} \frac{\phi_a}{m} \chi_1 \rho^2 \right] \delta_{ik} \\ & + \left[1 + \frac{2}{5} \frac{2\pi}{3} \frac{a^3}{m} \rho Y \right] \sigma_{ik} \\ & - \frac{4}{5} \frac{a^4 \sqrt{\pi}}{m} \frac{\rho^2 Y}{\sqrt{\theta}} \left(\theta \frac{\partial \delta_{(ik} v_s)}{\partial x_s} + \frac{1}{10} \frac{\partial \delta_{(ik} q_s)}{\rho} + \frac{1}{42} \frac{\partial m_{iks}}{\rho} \right) \\ & + \frac{\pi}{60} \frac{a^5}{m} \left(\frac{\partial^2 Y \rho^2 \theta}{\partial x_s \partial x_t} + 3Y \frac{\partial^2 \rho^2 \theta}{\partial x_s \partial x_t} - 12Y \frac{\partial \rho}{\partial x_s} \frac{\partial \rho \theta}{\partial x_t} \right) \delta_{(ik} \delta_{st)} \\ & - \frac{2\pi}{15} \frac{a^5}{m} \phi_a \chi_3 \left[\left(\rho \frac{\partial^2 \rho}{\partial x_r \partial x_r} + \frac{1}{2} \frac{\partial \rho}{\partial x_r} \frac{\partial \rho}{\partial x_r} \right) \delta_{ik} - \frac{\partial \rho}{\partial x_i} \frac{\partial \rho}{\partial x_k} \right] \end{aligned} \right) = \rho G_i. \tag{6.2}$$

This equation has the usual form of the momentum balance,

$$\rho \frac{Dv_i}{Dt} + \frac{\partial (p \delta_{ik} + \Pi_{ik})}{\partial x_k} = \rho G_i, \tag{6.3}$$

with a generalized stress tensor $p\delta_{ik} + \Pi_{ik}$ that has many contributions that can be read from (6.2). The first line describes the van-der-Waals-like pressure

$$p = \rho\theta \left(1 + \frac{2\pi}{3} \frac{a^3}{m} \rho Y \right) - \frac{2\pi a^3}{3} \frac{\phi_a}{m} \chi_1 \rho^2, \tag{6.4}$$

with a volume correction stemming from the Enskog term, and the pressure-reducing Vlasov contribution. The remainder is the non-equilibrium stress Π_{ik} , where the second line is the contribution from kinetic stress σ_{ij} with a correction due to the Enskog term. The last line is the fifth-order Korteweg stress, which is corrected by the fifth-order Enskog terms in the preceding line. The third line describes higher contributions to stress, including a Navier–Stokes-like contribution from the velocity gradient, a Burnett-like term with the gradient of the kinetic heat flux (i.e. thermal stress), and a higher contribution with m_{ijk} .

In equilibrium, we have $v_i = \sigma_{ik} = q_k = m_{ijk} = \Delta = R_{ik} = 0$. Then the equilibrium density field follows from the first, fourth and fifth lines of (6.2). The solution allows for smooth phase interfaces, where the Korteweg stress stabilizes the non-monotonic van-der-Waals-like pressure. Details of one-dimensional interfaces are presented by Frezzotti *et al.* (2005).

6.3. Balance of thermal energy

The balance of thermal energy includes terms up to fourth order, with frictional heating:

$$\begin{aligned} & \frac{3}{2} \rho \frac{D\theta}{Dt} + \frac{\partial}{\partial x_k} \left[\begin{aligned} & \left(1 + \frac{3}{5} \frac{2\pi}{3} \frac{a^3}{m} \rho Y \right) q_k \\ & - \frac{a^4 \sqrt{\pi}}{m} \frac{\rho^2 Y}{\sqrt{\theta}} \left(\frac{2}{3} \theta \frac{\partial \theta}{\partial x_k} + \frac{4}{15} \theta \frac{\partial \sigma_{ks}}{\rho} + \frac{1}{90} \frac{\partial \Delta}{\rho} + \frac{2}{105} \frac{\partial R_{ks}}{\rho} \right) \end{aligned} \right] \\ & = - \left(\Pi_{kl} - \mathcal{T}_{rs}^K \right) \frac{\partial v_k}{\partial x_l}. \end{aligned} \tag{6.5}$$

This has the usual form of the balance of internal energy,

$$\frac{3}{2} \rho \frac{D\theta}{Dt} + \frac{\partial Q_k}{\partial x_k} = - \hat{\Pi}_{kl} \frac{\partial v_k}{\partial x_l}, \tag{6.6}$$

with a generalized heat flux Q_k that has several contributions that can be read from (6.5). The first line is the contribution from kinetic heat flux q_i with a correction due to the Enskog term. The second line describes higher contributions to heat flux, including a Fourier-like contribution from the temperature gradient, a Burnett-like term with the kinetic stress tensor σ_{ij} (non-Fourier heat flux), and higher-order contributions related to Δ and R_{ij} .

The energy exchange term on the right-hand side contains only the non-Vlasov stress tensor contribution $\hat{\Pi}_{kl} = (\Pi_{kl} - \mathcal{T}_{rs}^K)$ and not the full stress tensor Π_{kl} that appears in the balance of momentum. As discussed earlier, the Vlasov stresses appear in the balance of Korteweg energy (see (4.8)), but do not contribute to frictional heating.

As written in (6.5), the right-hand side contains nonlinear terms related to friction, but in the linear approximation used throughout, these are ignored, and the energy exchange reduces to the work for volume change:

$$-\hat{\Pi}_{kl} \frac{\partial v_k}{\partial x_l} = -\left(\Pi_{kl} - \mathcal{T}_{rs}^K\right) \frac{\partial v_k}{\partial x_l} \simeq -\rho\theta \left(1 + \frac{2\pi}{3} \frac{a^3}{m} \rho Y\right) \frac{\partial v_k}{\partial x_k}. \quad (6.7)$$

The balance of total energy has balance law form, with the total energy flux under the divergence. Within the EV model, one has to account for thermal, kinetic and Vlasov energy, and the equation reads, in compact form,

$$\rho \frac{D\left(\frac{3}{2}\theta + \frac{1}{2}v^2 + \epsilon_K\right)}{Dt} + \frac{\partial(Q_k + q_k^K + \Pi_{ik}v_i)}{\partial x_k} = \rho v_i G_i. \quad (6.8)$$

6.4. Stress balance

The linearized balance for the kinetic stress tensor includes a larger number of terms up to fourth order:

$$\begin{aligned} & \frac{\partial \sigma_{ij}}{\partial t} + 2 \left[\rho\theta \left(1 + \frac{2}{5} \frac{2\pi}{3} \frac{a^3}{m} \rho Y\right) \right] \frac{\partial v_{(i}}{\partial x_{j)}} + \frac{4}{5} \frac{\partial}{\partial x_{(i}} \left[\left(1 + \frac{3}{5} \frac{2\pi}{3} \frac{a^3}{m} \rho Y\right) q_{j)} \right] \\ & + \frac{\partial}{\partial x_k} \left[\left(1 + \frac{6}{35} \frac{2\pi}{3} \frac{a^3}{m} \rho Y\right) m_{ijk} \right] + \frac{2\pi}{3} \frac{a^3}{m} \left[\frac{6}{25} q_{(i} \delta_{j)r} + \frac{8}{35} m_{ijr} \right] \frac{1}{\rho} \frac{\partial \rho^2 Y}{\partial x_r} \\ & - \frac{\sqrt{\pi} a^4}{m} \sqrt{\theta} \left[\frac{8}{15} \rho^2 \frac{\partial}{\partial x_{(i}} \left(Y \frac{\partial \theta}{\partial x_{j)}} \right) + \frac{16}{15} \rho Y \frac{\partial \rho}{\partial x_{(i}} \frac{\partial \theta}{\partial x_{j)}} \right] \\ & - \frac{\sqrt{\pi} a^4}{m\sqrt{\theta}} \left[\frac{2}{225} \rho \frac{\partial}{\partial x_{(i}} \left(Y \frac{\partial \Delta}{\partial x_{j)}} \right) - \frac{2}{225} \Delta \frac{\partial}{\partial x_{(i}} \left(Y \frac{\partial \rho}{\partial x_{j)}} \right) \right] \\ & - \frac{\sqrt{\pi} a^4}{m} \sqrt{\theta} \left[\frac{8}{105} \rho \frac{\partial}{\partial x_r} \left(Y \frac{\partial \sigma_{ij}}{\partial x_r} \right) - \frac{16}{35} \sigma_{ij} \frac{\partial}{\partial x_r} \left(Y \frac{\partial \rho}{\partial x_r} \right) - \frac{2}{21} \rho \sigma_{ij} \frac{\partial^2 Y}{\partial x_r \partial x_r} \right] \\ & - \frac{\sqrt{\pi} a^4}{m} \sqrt{\theta} \left[\begin{aligned} & \frac{16}{105} \rho \frac{\partial}{\partial x_{(i}} \left(Y \frac{\partial \sigma_{j)r}}{\partial x_r} \right) + \frac{16}{105} \rho \frac{\partial}{\partial x_r} \left(Y \frac{\partial \sigma_{r(i}}{\partial x_{j)}} \right) \\ & - \frac{8}{21} \sigma_{r(i} \frac{\partial}{\partial x_{j)}} \left(Y \frac{\partial \rho}{\partial x_r} \right) - \frac{8}{21} \sigma_{r(i} \frac{\partial}{\partial x_r} \left(Y \frac{\partial \rho}{\partial x_{j)}} \right) - \frac{4}{35} \rho \sigma_{r(i} \frac{\partial^2 Y}{\partial x_{j)} \partial x_r} \end{aligned} \right] \\ & - \frac{\sqrt{\pi} a^4}{m\sqrt{\theta}} \left[\frac{4}{735} \rho \frac{\partial}{\partial x_r} \left(Y \frac{\partial R_{ij}}{\partial x_r} \right) - \frac{2}{105} R_{ij} \frac{\partial}{\partial x_r} \left(Y \frac{\partial \rho}{\partial x_r} \right) - \frac{1}{294} \rho R_{ij} \frac{\partial^2 Y}{\partial x_r \partial x_r} \right] \\ & - \frac{\sqrt{\pi} a^4}{m\sqrt{\theta}} \left[\begin{aligned} & \frac{8}{735} \rho \frac{\partial}{\partial x_{(i}} \left(Y \frac{\partial R_{j)r}}{\partial x_r} \right) + \frac{8}{735} \rho \frac{\partial}{\partial x_r} \left(Y \frac{\partial R_{r(i}}{\partial x_{j)}} \right) \\ & - \frac{2}{105} R_{r(i} \frac{\partial}{\partial x_r} \left(Y \frac{\partial \rho}{\partial x_{j)}} \right) - \frac{2}{105} R_{r(i} \frac{\partial}{\partial x_{j)}} \left(Y \frac{\partial \rho}{\partial x_r} \right) - \frac{1}{245} \rho R_{r(i} \frac{\partial^2 Y}{\partial x_{j)} \partial x_r} \end{aligned} \right] \\ & = - \left[\frac{16}{5} \frac{\rho \sqrt{\pi \theta} a^2}{m} Y \right] \left(\sigma_{ij} + \frac{1}{28} \frac{R_{ij}}{\theta} \right). \quad (6.9) \end{aligned}$$

6.5. Heat flux balance

The linearized balance for kinetic energy flux also includes many terms up to fourth order:

$$\begin{aligned}
 & \frac{\partial q_i}{\partial t} + \frac{5}{2} \rho \theta \left(1 + \frac{3}{5} \frac{2\pi}{3} \frac{a^3}{m} \rho Y \right) \frac{\partial \theta}{\partial x_i} + \theta \frac{\partial}{\partial x_k} \left[\left(1 + \frac{3}{5} \frac{2\pi}{3} \frac{a^3}{m} \rho Y \right) \sigma_{ik} \right] \\
 & + \frac{1}{2} \frac{\partial}{\partial x_k} \left[\left(1 + \frac{12}{35} \frac{2\pi}{3} \frac{a^3}{m} \rho Y \right) R_{ik} \right] + \frac{1}{6} \frac{\partial}{\partial x_i} \left[\left(1 + \frac{3}{5} \frac{2\pi}{3} \frac{a^3}{m} \rho Y \right) \Delta \right] \\
 & - \frac{\sigma_{ik}}{\rho} \theta \frac{\partial}{\partial x_k} \left[\left(1 + \frac{9}{10} \frac{2\pi}{3} \frac{a^3}{m} \rho Y \right) \rho \right] + \frac{2\pi}{3} \frac{a^3}{m} \left[\frac{1}{30} \frac{\Delta}{\rho} \delta_{ik} + \frac{11}{140} \frac{R_{ik}}{\rho} \right] \frac{\partial \rho^2 Y}{\partial x_k} \\
 & - \frac{\sqrt{\pi} a^4}{m} \sqrt{\theta} \left[-\frac{19}{15} \theta \frac{\partial}{\partial x_r} \left(\rho^2 Y \frac{\partial v_i}{\partial x_r} \right) - \frac{38}{15} \theta \frac{\partial}{\partial x_{(i}} \left(\rho^2 Y \frac{\partial v_r}{\partial x_r} \right) \right] \\
 & - \frac{\sqrt{\pi} a^4}{m} \sqrt{\theta} \left[\frac{9}{50} \rho \frac{\partial}{\partial x_r} \left(Y \frac{\partial q_i}{\partial x_r} \right) - \frac{1}{2} q_i \frac{\partial}{\partial x_r} \left(Y \frac{\partial \rho}{\partial x_r} \right) - \frac{2}{25} \rho q_i \frac{\partial^2 Y}{\partial x_r \partial x_r} \right] \\
 & - \frac{\sqrt{\pi} a^4}{m} \sqrt{\theta} \left[\frac{9}{25} \rho \frac{\partial}{\partial x_{(i}} \left(Y \frac{\partial q_r}{\partial x_r} \right) - \frac{11}{15} q_r \frac{\partial}{\partial x_{(i}} \left(Y \frac{\partial \rho}{\partial x_r} \right) - \frac{2}{75} \rho q_r \frac{\partial^2 Y}{\partial x_r \partial x_i} \right] \\
 & - \frac{\sqrt{\pi} a^4}{m} \sqrt{\theta} \left[\frac{9}{70} \rho \frac{\partial}{\partial x_r} \left(Y \frac{\partial m_{irs}}{\partial x_s} \right) - \frac{1}{6} m_{irs} \frac{\partial}{\partial x_r} \left(Y \frac{\partial \rho}{\partial x_s} \right) - \frac{1}{105} \rho m_{irs} \frac{\partial^2 Y}{\partial x_r \partial x_s} \right] \\
 & = -\frac{2}{3} \left[\frac{16}{5} \frac{\rho \sqrt{\pi \theta} a^2}{m} Y \right] q_i. \tag{6.10}
 \end{aligned}$$

6.6. m_{ijk} balance

The linearized transport equation up to fourth order reads

$$\begin{aligned}
 & \frac{\partial m_{ijk}}{\partial t} + 3\theta \frac{\partial}{\partial x_{(i}} \left[\left(1 + \frac{6}{35} \frac{2\pi}{3} \frac{a^3}{m} \rho Y \right) \sigma_{jk)} \right] - 3 \frac{\theta \sigma_{(ij}}{\rho} \frac{\partial}{\partial x_k)} \left[\rho + \frac{2}{5} \frac{2\pi}{3} \frac{a^3}{m} \rho^2 Y \right] \\
 & + \frac{3}{7} \frac{\partial}{\partial x_{(i}} \left[\left(1 + \frac{12}{35} \frac{2\pi}{3} \frac{a^3}{m} \rho Y \right) R_{jk)} \right] + \frac{93}{490} \frac{2\pi}{3} \frac{a^3}{m} \frac{R_{(ij}}{\rho} \frac{\partial \rho^2 Y}{\partial x_k)} \\
 & - \frac{\sqrt{\pi} a^4}{m} \sqrt{\theta} \left[\frac{4}{35} \theta \frac{\partial}{\partial x_{(i}} \left(\rho^2 Y \frac{\partial v_j}{\partial x_k)} \right) \right] \\
 & - \frac{\sqrt{\pi} a^4}{m} \sqrt{\theta} \left[\frac{54}{175} \rho \frac{\partial}{\partial x_{(i}} \left(Y \frac{\partial q_j}{\partial x_k)} \right) - \frac{2}{5} q_{(i} \frac{\partial}{\partial x_j} \left(Y \frac{\partial \rho}{\partial x_k)} \right) - \frac{4}{175} \rho q_{(i} \frac{\partial^2 Y}{\partial x_j \partial x_k)} \right] \\
 & - \frac{\sqrt{\pi} a^4}{m} \sqrt{\theta} \left[\frac{2}{70} \rho \frac{\partial}{\partial x_r} \left(Y \frac{\partial m_{ijk}}{\partial x_r} \right) - \frac{3}{5} m_{ijk} \frac{\partial}{\partial x_r} \left(Y \frac{\partial \rho}{\partial x_r} \right) - \frac{1}{7} \rho m_{ijk} \frac{\partial^2 Y}{\partial x_r \partial x_r} \right] \\
 & - \frac{\sqrt{\pi} a^4}{m} \sqrt{\theta} \left[\frac{6}{70} \rho \frac{\partial}{\partial x_{(i}} \left(Y \frac{\partial m_{jk)r}}{\partial x_r} \right) - \frac{3}{7} m_{r(ij} \frac{\partial}{\partial x_k)} \left(Y \frac{\partial \rho}{\partial x_r} \right) - \frac{3}{35} \rho m_{r(ij} \frac{\partial^2 Y}{\partial x_k \partial x_r} \right]
 \end{aligned}$$

Twenty-six moment equations for the Enskog–Vlasov equation

$$\begin{aligned}
 & -\frac{\sqrt{\pi}a^4}{m}\sqrt{\theta}\left[\frac{6}{70}\rho\frac{\partial}{\partial x_r}\left(Y\frac{\partial m_{r(ij)}}{\partial x_k}\right)-\frac{3}{7}m_{r(ij)}\frac{\partial}{\partial x_r}\left(Y\frac{\partial\rho}{\partial x_k}\right)-\frac{3}{35}\rho m_{r(ij)}\frac{\partial^2 Y}{\partial x_k\partial x_r}\right] \\
 & =-\frac{3}{2}\left[\frac{16}{5}\frac{\rho\sqrt{\pi\theta}a^2}{m}Y\right]m_{ijk}.
 \end{aligned} \tag{6.11}$$

6.7. Δ balance

The linearized transport equation up to fourth order reads

$$\begin{aligned}
 & \frac{D\Delta}{Dt}+8\theta\frac{\partial}{\partial x_k}\left[\left(1+\frac{3}{5}\frac{2\pi}{3}\frac{a^3}{m}\rho Y\right)q_k\right]-8\theta\frac{q_k}{\rho}\frac{\partial}{\partial x_k}\left[\left(1+\frac{4}{5}\frac{2\pi}{3}\frac{a^3}{m}\rho Y\right)\rho\right] \\
 & -\frac{a^4\sqrt{\pi}}{m}\sqrt{\theta}\left[\frac{4}{3}\rho^2\theta\frac{\partial}{\partial x_r}\left(Y\frac{\partial\theta}{\partial x_r}\right)+\frac{8}{3}\theta\rho Y\frac{\partial\rho}{\partial x_r}\frac{\partial\theta}{\partial x_r}\right] \\
 & -\frac{a^4\sqrt{\pi}}{m}\sqrt{\theta}\left[\frac{8}{15}\rho^2\theta\frac{\partial}{\partial x_r}\left(Y\frac{\partial\sigma_{rs}}{\partial x_s}\right)-\frac{32}{3}\rho\theta Y\frac{\partial\rho}{\partial x_r}\frac{\partial\sigma_{rs}}{\partial x_s}\right] \\
 & -\frac{a^4\sqrt{\pi}}{m}\sqrt{\theta}\left[\frac{1}{3}\rho\frac{\partial}{\partial x_r}\left(Y\frac{\partial\Delta}{\partial x_r}\right)-\frac{31}{45}\Delta\frac{\partial}{\partial x_r}\left(Y\frac{\partial\rho}{\partial x_r}\right)-\frac{4}{45}\Delta\rho\frac{\partial^2 Y}{\partial x_r\partial x_r}\right] \\
 & -\frac{a^4\sqrt{\pi}}{m}\sqrt{\theta}\left[\frac{4}{7}\rho\frac{\partial}{\partial x_r}\left(Y\frac{\partial R_{rs}}{\partial x_s}\right)-\frac{76}{105}R_{rs}\frac{\partial}{\partial x_r}\left(Y\frac{\partial\rho}{\partial x_s}\right)-\frac{4}{105}\rho R_{rs}\frac{\partial^2 Y}{\partial x_r\partial x_s}\right] \\
 & =-\frac{2}{3}\left[\frac{16}{5}\frac{a^2\rho\sqrt{\pi\theta}}{m}Y\right]\Delta.
 \end{aligned} \tag{6.12}$$

6.8. R_{ij} balance

The linearized transport equation up to fourth order reads

$$\begin{aligned}
 & \frac{\partial R_{ij}}{\partial t}+\frac{28}{5}\theta\frac{\partial}{\partial x_{(i}}\left[\left(1+\frac{12}{35}\frac{2\pi}{3}\frac{a^3}{m}\rho Y\right)q_{j)}\right]-\frac{28}{5}\theta\frac{q_{(i}}{\rho}\frac{\partial}{\partial x_{j)}}\left[\left(1+\frac{1}{2}\frac{2\pi}{3}\frac{a^3}{m}\rho Y\right)\rho\right] \\
 & +2\theta\frac{\partial}{\partial x_k}\left[\left(1+\frac{12}{35}\frac{2\pi}{3}\frac{a^3}{m}\rho Y\right)m_{ijk}\right]-2\frac{m_{ijk}\theta}{\rho}\frac{\partial}{\partial x_k}\left[\left(1+\frac{11}{14}\frac{2\pi}{3}\frac{a^3}{m}\rho Y\right)\rho\right] \\
 & -\frac{\sqrt{\pi}a^4}{m}\sqrt{\theta}\left[\frac{8}{15}\rho^2\theta\frac{\partial}{\partial x_{(i}}\left(Y\frac{\partial\theta}{\partial x_{j)}}\right)+\frac{16}{15}\rho\theta Y\frac{\partial\rho}{\partial x_{(i}}\frac{\partial\theta}{\partial x_{j)}}\right] \\
 & -\frac{a^4\sqrt{\pi}}{m}\sqrt{\theta}\left[\frac{2}{15}\rho\frac{\partial}{\partial x_{(i}}\left(Y\frac{\partial\Delta}{\partial x_{j)}}\right)-\frac{38}{225}\Delta\frac{\partial}{\partial x_{(i}}\left(Y\frac{\partial\rho}{\partial x_{j)}}\right)-\frac{2}{225}\rho\Delta\frac{\partial^2 Y}{\partial x_{(i}}\frac{\partial x_{j)}}\right] \\
 & -\frac{a^4\sqrt{\pi}}{m}\sqrt{\theta}\left[\frac{8}{105}\rho\theta\frac{\partial}{\partial x_r}\left(Y\frac{\partial\sigma_{ij}}{\partial x_r}\right)-\frac{4}{15}\theta\sigma_{ij}\frac{\partial}{\partial x_r}\left(Y\frac{\partial\rho}{\partial x_r}\right)-\frac{1}{21}\rho\theta\sigma_{ij}\frac{\partial^2 Y}{\partial x_r\partial x_r}\right]
 \end{aligned}$$

$$\begin{aligned}
 & -\frac{a^4\sqrt{\pi}}{m}\sqrt{\theta} \left[\begin{aligned} & \frac{16}{105}\rho\theta \frac{\partial}{\partial x_{(i}} \left(Y \frac{\partial\sigma_{j)r}}{\partial x_r} \right) + \frac{16}{105}\rho\theta \frac{\partial}{\partial x_r} \left(Y \frac{\partial\sigma_{r(i}}{\partial x_{j)}} \right) \\ & -\frac{4}{15}\theta\sigma_{r(i} \frac{\partial}{\partial x_{j)}} \left(Y \frac{\partial\rho}{\partial x_r} \right) - \frac{4}{15}\theta\sigma_{r(i} \frac{\partial}{\partial x_r} \left(Y \frac{\partial\rho}{\partial x_{j)}} \right) \\ & \qquad\qquad\qquad -\frac{2}{35}\rho\theta\sigma_{r(i} \frac{\partial^2 Y}{\partial x_{j)}\partial x_r} \end{aligned} \right] \\
 & -\frac{a^4\sqrt{\pi}}{m}\sqrt{\theta} \left[\begin{aligned} & \frac{4}{49}\rho \frac{\partial}{\partial x_r} \left(Y \frac{\partial R_{ij}}{\partial x_r} \right) - \frac{149}{245}R_{ij} \frac{\partial}{\partial x_r} \left(Y \frac{\partial\rho}{\partial x_r} \right) - \frac{129}{980}\rho R_{ij} \frac{\partial^2 Y}{\partial x_r\partial x_r} \end{aligned} \right] \\
 & -\frac{a^4\sqrt{\pi}}{m}\sqrt{\theta} \left[\begin{aligned} & \frac{8}{49}\rho \frac{\partial}{\partial x_{(i}} \left(Y \frac{\partial R_{j)r}}{\partial x_r} \right) + \frac{8}{49}\rho \frac{\partial}{\partial x_r} \left(Y \frac{\partial R_{r(i}}{\partial x_{j)}} \right) \\ & -\frac{257}{735}R_{r(i} \frac{\partial}{\partial x_{j)}} \left(Y \frac{\partial\rho}{\partial x_r} \right) - \frac{257}{735}R_{r(i} \frac{\partial}{\partial x_r} \left(Y \frac{\partial\rho}{\partial x_{j)}} \right) \\ & \qquad\qquad\qquad -\frac{137}{1470}\rho R_{r(i} \frac{\partial^2 Y}{\partial x_{j)}\partial x_r} \end{aligned} \right] \\
 & = -\left[\frac{16}{5} \frac{a^2\rho\sqrt{\pi\theta}}{m} Y \right] \left(\frac{1}{2}\theta\sigma_{ij} + \frac{205}{168}R_{ij} \right). \tag{6.13}
 \end{aligned}$$

6.9. Ideal gas limit

The above equations are valid, within the limitations of the underlying theory, for all states from compressed liquid over two-phase flows and real gas, to ideal gas. For the case of the latter, they agree with the Grad 26 moment equations as presented in Struchtrup (2005) within the limits of the performed linearizations. Indeed, the ideal gas case of the above is obtained from (6.1)–(6.13) by removing all terms with powers a^3 and higher, and setting $Y = 1$ (with $p = \rho\theta$, $1/\tau = \frac{16}{5}(\rho\sqrt{\pi\theta}a^2/m)$), as

$$\left. \begin{aligned}
 & \frac{\partial\rho}{\partial t} + \frac{\partial\rho v_k}{\partial x_k} = 0, \\
 & \rho \frac{Dv_i}{Dt} + \frac{\partial}{\partial x_k} (\rho\theta\delta_{ik} + \sigma_{ik}) = \rho G_i, \\
 & \frac{3}{2}\rho \frac{D\theta}{Dt} + \frac{\partial q_k}{\partial x_k} = -\rho\theta \frac{\partial v_k}{\partial x_k}, \\
 & \frac{\partial\sigma_{ij}}{\partial t} + 2\rho\theta \frac{\partial v_{(i}}{\partial x_{j)}} + \frac{4}{5} \frac{\partial q_{(i}}{\partial x_{j)}} + \frac{\partial m_{ijk}}{\partial x_k} = -\frac{1}{\tau} \left(\sigma_{ij} + \frac{1}{28} \frac{R_{ij}}{\theta} \right), \\
 & \frac{\partial q_i}{\partial t} + \frac{5}{2}\rho\theta \frac{\partial\theta}{\partial x_i} + \theta \frac{\partial\sigma_{ik}}{\partial x_k} - \theta\sigma_{ik} \frac{\partial \ln \rho}{\partial x_k} + \frac{1}{2} \frac{\partial R_{ik}}{\partial x_k} + \frac{1}{6} \frac{\partial \Delta}{\partial x_i} = -\frac{2}{3} \frac{q_i}{\tau}, \\
 & \frac{\partial m_{ijk}}{\partial t} + 3\theta \frac{\partial\sigma_{(ij}}{\partial x_{k)}} + \frac{3}{7} \frac{\partial R_{(ij}}{\partial x_{k)}} - 3\theta\sigma_{(ij} \frac{\partial \ln \rho}{\partial x_{k)}} = -\frac{3}{2} \frac{m_{ijk}}{\tau}, \\
 & \frac{\partial \Delta}{\partial t} + 8\theta \frac{\partial q_k}{\partial x_k} - 8\theta q_k \frac{\partial \ln \rho}{\partial x_k} = -\frac{2}{3} \frac{\Delta}{\tau}, \\
 & \frac{\partial R_{ij}}{\partial t} + \frac{28}{5}\theta \frac{\partial q_{(i}}{\partial x_{j)}} - \frac{28}{5}\theta q_{(i} \frac{\partial \ln \rho}{\partial x_{j)}} - 2m_{ijk}\theta \frac{\partial \ln \rho}{\partial x_k} + 2\theta \frac{\partial m_{ijk}}{\partial x_k} = -\frac{1}{\tau} \left(\frac{1}{2}\theta\sigma_{ij} + \frac{205}{168}R_{ij} \right).
 \end{aligned} \right\} \tag{6.14}$$

Comparison with the equations in Chapter 9 of Struchtrup (2005) shows that the above without the underlined terms are the linearized version of the Grad 26 equations for the ideal gas. The underlined terms are nonlinear with the density gradient and appear in the nonlinear Grad 26 equations, which, however, contain other nonlinear terms that were removed during the above derivation. The collision terms here are for a hard-sphere gas, while in Struchtrup (2005) they are given for Maxwell molecules.

6.10. Wall boundary conditions

The EV26 equations presented above ((6.1), (6.2), (6.5), (6.9)–(6.13)) contain many terms with higher derivatives. For the computation of boundary-value problems, they must be furnished with appropriate boundary conditions.

Development of boundary conditions for the ideal gas moment equations is well understood; e.g. see Torrillon & Struchtrup (2008) and Torrillon (2016), with moment boundary conditions developed from boundary conditions for the Boltzmann equation and the Grad distribution function.

A similar approach is expected to find boundary conditions for EV26. However, due to the higher-order derivatives appearing in the equations, as a result of the Taylor expansions (essentially the terms with a^4), it is expected that EV26 requires a larger number of boundary conditions than Grad26 (or R13).

Sufficiently far from the interface and walls, the bulk liquid and vapour behaviour are governed by the classical NSF laws. For studying non-equilibrium phase interfaces far from walls, it suffices to impose the NSF equations at the system boundary. This approach is used in results presented below.

Classical kinetic theory boundary conditions are effectively based on impulsive wall scattering models (Cercignani 1975), and do not consider Vlasov like long-distance interaction between wall and a vapour or liquid particle. Hence both the kinetic boundary conditions for the EV equation and the development of a complete set of boundary conditions for its 26 moments approximation will require further thought.

7. Two-phase processes

The above list (6.1)–(6.13) of transport equations is rather rich. Analytical and numerical solutions for a variety of problems are required to evaluate the physics described. Such detailed solutions of the equations for processes involving interfaces, and their discussion, will be presented elsewhere.

For solutions of the 26 moment equations for the EV equation, it is convenient to chose units such that

$$a = m = \phi_a = 1. \tag{7.1}$$

With this, length x is measured in multiples of a , density ρ in multiples of m/a^3 , temperature $\theta = RT$ in multiples of ϕ_a , and time t in multiples of $a/\sqrt{\phi_a}$. Moreover, data and figures shown below are for power potentials with $\gamma = 6$, such that $\chi_1 = \gamma/(\gamma - 3) = 2$ and $\chi_3 = \gamma/(\gamma - 5) = 6$.

7.1. Equilibrium

For additional context, we will have a brief look at equilibrium rest states, where all time derivatives vanish, and we expect homogeneous temperature, and vanishing

non-equilibrium variables, so that

$$\frac{\partial \theta}{\partial x_i} = v_i = \sigma_{ij} = q_i = m_{ijk} = \Delta = R_{ij} = 0. \quad (7.2)$$

Then apart from the momentum balance, all equations are identically fulfilled. In a one-dimensional setting, where $\rho = \rho(x)$, the momentum balance reduces to an equation for density (no body force G_i):

$$\frac{\partial}{\partial x} \left\{ \begin{aligned} & \rho \theta \left(1 + \frac{2\pi}{3} \rho Y \right) - \frac{2\pi a^3}{3} \chi_1 \rho^2 \\ & + \frac{\pi}{60} \theta \left[\frac{\partial^2 Y \rho^2}{\partial x \partial x} + 3Y \left(\frac{\partial^2 \rho^2}{\partial x \partial x} - 4 \frac{\partial \rho}{\partial x} \frac{\partial \rho}{\partial x} \right) \right] - \frac{2\pi}{15} \chi_3 \left(\rho \frac{\partial^2 \rho}{\partial x \partial x} - \frac{1}{2} \frac{\partial \rho}{\partial x} \frac{\partial \rho}{\partial x} \right) \end{aligned} \right\} = 0. \quad (7.3)$$

That is, the divergence of the overall normal stress $\{\bullet\}$ (the expression between the braces in (7.3)) vanishes. This equation allows phase equilibrium between saturated liquid and vapour phases, with continuous density variation across the interface.

For the case without interface, that is, for a single phase, the gradients of density vanish, and the pressure

$$p = \rho \theta \left(1 + \frac{2\pi}{3} \rho Y \right) - \frac{2\pi}{3} \chi_1 \rho^2 \quad (7.4)$$

is homogeneous.

It is well known that van-der-Waals-like equations of state such as this are non-monotonic, and allow for phase equilibrium (Struchtrup 2014). We denote the specific volume as $v = 1/\rho$. The critical point is found from the condition for a horizontal inflection point in the p - v diagram,

$$\left(\frac{\partial p}{\partial v} \right)_{\theta, crit} = \left(\frac{\partial^2 p}{\partial v^2} \right)_{\theta, crit} = 0, \quad (7.5)$$

as

$$\theta_{crit} = 0.7546, \quad p_{crit} = 0.06748, \quad v_{crit} = 4.014. \quad (7.6a-c)$$

For subcritical temperatures, $\theta < \theta_{crit}$, equilibrium solutions exist, where a continuous interface connects two homogeneous regions at different mass densities – these are the states of saturated liquid and vapour, which both are at the unique saturation pressure $p_{sat}(\theta)$. As an example, figure 1 shows the liquid–vapour equilibrium for a system of length $L = 40$ at temperature $\theta = 0.65$, obtained from numerical solution of (7.3). The location of the interface depends on the average density $\bar{\rho} = (1/L) \int_0^L \rho \, dx$ of the system, which must lie between the saturated liquid and vapour densities, $\rho_V < \bar{\rho} < \rho_L$.

According to (7.3), the overall normal stress is a constant. The pressure $p(\theta, \rho)$ of (7.4), however, varies throughout the interface, as shown in figure 2, where it is balanced by the Korteweg stresses. The pressure in the bulk phases, and hence the overall stress, equals the saturation pressure p_{sat} , as indicated in the figure.

Solving (7.3) at other subcritical temperatures gives a complete set of data for saturation pressure $p_{sat}(\theta)$ and the corresponding saturated liquid and vapour volumes $v_L(\theta) = 1/\rho_L(\theta)$ and $v_V(\theta) = 1/\rho_V(\theta)$. These are collected in the p - v diagram of figure 3, which shows the saturated liquid and vapour lines.

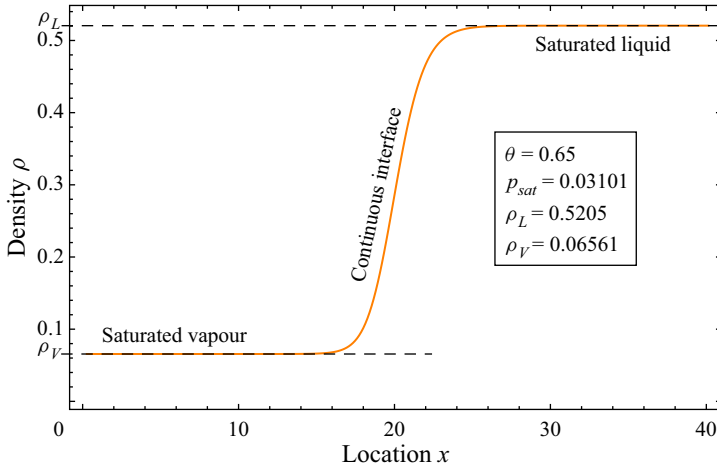


Figure 1. Density profile in liquid–vapour equilibrium for $\theta = 0.65$.

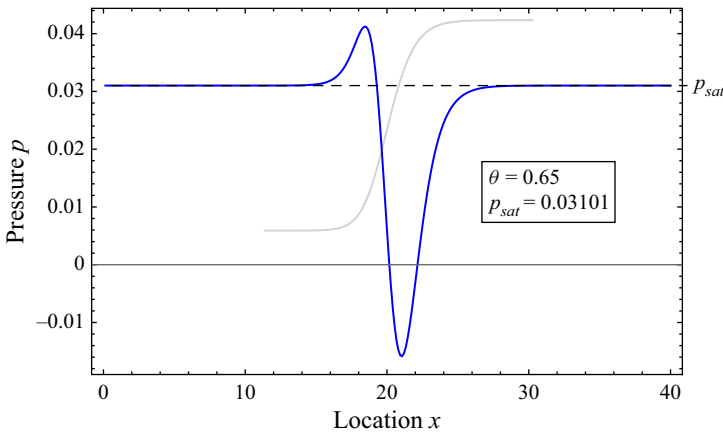


Figure 2. Pressure profile $p(\theta, \rho)$ over the interface. The density curve is underlaid to identify the location of the liquid–vapour interface.

The p – v diagram also shows the isotherms of pressure $p(\theta, v)$ of (7.4) with the well-known non-monotonic shape of the subcritical isotherm (e.g. $\theta = 0.65$). Thermodynamic stability requires $(\partial p / \partial v)_\theta < 0$ (Struchtrup 2014), hence the pressure (7.4) alone is not stable. The interface is stabilized through the Korteweg stresses in (7.3), which balance the non-monotonic parts of the pressure, resulting in the continuous interface structure shown in figure 1.

We note that the determination of the saturation state for the EV gas relies on the evaluation of the balance of momentum (7.3). The typical thermodynamic argument employs Maxwell’s equal area rule (Struchtrup 2014), where the saturation state follows from the condition

$$\int_L^V p(\theta, v) \, dv = p_{sat} (v_V - v_L). \quad (7.7)$$

For $\theta = 0.65$, the equal area rule gives $p_{sat} = 0.03098$, $\rho_L = 0.5205$, $\rho_V = 0.06552$; in comparison, the EV results have minute relative errors of 0.09 %, 0.13 %, 0.005 %.

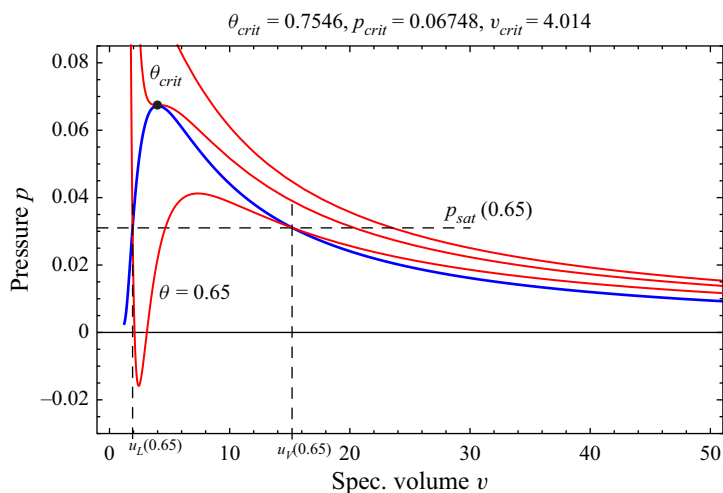


Figure 3. Saturation curve (blue) and three isothermal lines $p(\theta, v)$ (red) in the p - v diagram. Saturated liquid and vapour volumes v_L and v_V , and saturation pressure p_{sat} , are indicated for $\theta = 0.65$. The black dot is the critical point.

Thermodynamic equilibrium requires that the Gibbs free energies of both phases agree, and this implies the equal area rule (Struchtrup 2014). Hence the equations as derived stand in (slight) contradiction to thermodynamics. Aifantis & Serrin (1983) presented a condition on capillary stress terms to agree with the equal area rule. Evaluation shows that the capillary stresses from the Vlasov term fulfil the condition, but the fifth-order Enskog contributions do not. A small *ad hoc* correction to the Enskog stress term of the form

$$P_{ij,correction} = \frac{\pi}{60} \frac{a^5}{m} \left(-\frac{1}{2} \theta \rho^2 \frac{d^2 Y}{d\rho^2} \frac{\partial \rho}{\partial x_s} \frac{\partial \rho}{\partial x_t} \right) \delta_{(ik} \delta_{st)} \quad (7.8)$$

suffices to retrieve the equal area rule; see Appendix C.

7.2. Isothermal Couette flow

As a first test for the set of 26 moment equations for the EV equation, we show a numerical solution for the case of a steady two-phase and isothermal Couette flow (Rah & Eu 2001; Frezzotti & Rossi 2012), along a liquid–vapour interface, where we compare results to a direct simulation Monte Carlo (DSMC). In the considered test problem, an infinite and planar liquid film, of nominal thickness x_l , is in contact with its vapour, through the liquid–vapour interface. A shear flow is induced in the two-phase system in such a way that, everywhere in the flow field, the velocity has a constant direction, parallel to the vapour liquid interface. Specifically, we use a coordinate system such that the interface normal points in the x_1 direction and the liquid film occupies the region $\mathcal{L} = \{(x_1, x_2, x_3) \in R^3 : 0 \leq x_1 < x_l\}$. The velocity, which only has component $v_2(x_1)$, is assumed to be zero at $x_1 = 0$, and to have constant gradient $\partial v_2 / \partial x_1 = \alpha$ far from the interface. Frictional heating is proportional to α^2 and can be ignored in the linearized approximation, assuming infinitely small shear rate. Hence the transport equations can be solved for the isothermal case, where specifically,

$$\frac{\partial \theta}{\partial x} = \Delta = 0. \quad (7.9)$$

Then the only non-vanishing variables are

$$\{\rho(x), v_2(x), \sigma_{12}(x), q_2(x), m_{112}(x), R_{12}(x)\}. \quad (7.10)$$

Within the approximations used, the density $\rho(x)$ is undisturbed and remains at the equilibrium solution, as given by (7.3), solely determined by the assumed temperature and liquid film thickness. The other variables assume non-equilibrium values, governed by the following set of linear differential equations, in which x_1 has been renamed x .

Momentum conservation, direction x_2 :

$$\begin{aligned} \frac{\partial}{\partial x} \left[\left(1 + \frac{2}{5} \frac{2\pi}{3} \frac{a^3}{m} \rho Y \right) \sigma_{12} \right. \\ \left. - \frac{a^4 \sqrt{\pi}}{m} \frac{\rho^2 Y}{\sqrt{\theta}} \left(\frac{4}{15} \theta \frac{\partial v_2}{\partial x} + \frac{2}{75} \frac{\partial}{\partial x} \left(\frac{q_2}{\rho} \right) + \frac{2}{105} \frac{\partial}{\partial x} \left(\frac{m_{112}}{\rho} \right) \right) \right] = 0. \end{aligned} \quad (7.11)$$

Balance equation for kinetic shear stress σ_{12} :

$$\begin{aligned} \left[\rho \theta \left(1 + \frac{2}{5} \frac{2\pi}{3} \frac{a^3}{m} \rho Y \right) \right] \frac{\partial v_2}{\partial x} + \frac{2}{5} \frac{\partial}{\partial x} \left[\left(1 + \frac{3}{5} \frac{2\pi}{3} \frac{a^3}{m} \rho Y \right) q_2 \right] \\ + \frac{\partial}{\partial x} \left[\left(1 + \frac{6}{35} \frac{2\pi}{3} \frac{a^3}{m} \rho Y \right) m_{112} \right] + \frac{2\pi}{3} \frac{a^3}{m} \left[\frac{3}{25} q_2 + \frac{8}{35} m_{112} \right] \frac{1}{\rho} \frac{\partial \rho^2 Y}{\partial x} \\ - \frac{\sqrt{\pi} a^4}{m} \sqrt{\theta} \left[\frac{8}{35} \rho \frac{\partial}{\partial x} \left(Y \frac{\partial \sigma_{12}}{\partial x} \right) - \frac{88}{105} \sigma_{12} \frac{\partial}{\partial x} \left(Y \frac{\partial \rho}{\partial x} \right) - \frac{16}{105} \rho \sigma_{12} \frac{\partial^2 Y}{\partial x^2} \right] \\ - \frac{\sqrt{\pi} a^4}{m \sqrt{\theta}} \left[\frac{4}{245} \rho \frac{\partial}{\partial x} \left(Y \frac{\partial R_{12}}{\partial x} \right) - \frac{4}{105} R_{12} \frac{\partial}{\partial x} \left(Y \frac{\partial \rho}{\partial x} \right) - \frac{4}{735} \rho R_{12} \frac{\partial^2 Y}{\partial x^2} \right] \\ = - \left[\frac{16}{5} \frac{\rho \sqrt{\pi \theta} a^2}{m} Y \right] \left(\sigma_{12} + \frac{1}{28} \frac{R_{12}}{\theta} \right). \end{aligned} \quad (7.12)$$

Balance equation for kinetic heat flux component q_2 :

$$\begin{aligned} \theta \frac{\partial}{\partial x} \left[\left(1 + \frac{3}{5} \frac{2\pi}{3} \frac{a^3}{m} \rho Y \right) \sigma_{12} \right] - \frac{\sigma_{12}}{\rho} \theta \frac{\partial}{\partial x} \left[\left(1 + \frac{9}{10} \frac{2\pi}{3} \frac{a^3}{m} \rho Y \right) \rho \right] \\ + \frac{1}{2} \frac{\partial}{\partial x} \left[\left(1 + \frac{12}{35} \frac{2\pi}{3} \frac{a^3}{m} \rho Y \right) R_{12} \right] + \frac{2\pi}{3} \frac{a^3}{m} \frac{11}{140} \frac{R_{12}}{\rho} \frac{\partial \rho^2 Y}{\partial x} \\ + \frac{\sqrt{\pi} a^4}{m} \sqrt{\theta} \frac{19}{15} \theta \left[\frac{\partial}{\partial x} \left(\rho^2 Y \frac{\partial v_2}{\partial x} \right) \right] \\ - \frac{\sqrt{\pi} a^4}{m} \sqrt{\theta} \left[\frac{9}{50} \rho \frac{\partial}{\partial x} \left(Y \frac{\partial q_2}{\partial x} \right) - \frac{1}{2} q_2 \frac{\partial}{\partial x} \left(Y \frac{\partial \rho}{\partial x} \right) - \frac{2}{25} \rho q_2 \frac{\partial^2 Y}{\partial x^2} \right] \\ - \frac{\sqrt{\pi} a^4}{m} \sqrt{\theta} \left[\frac{9}{70} \rho \frac{\partial}{\partial x} \left(Y \frac{\partial m_{112}}{\partial x} \right) - \frac{1}{6} m_{112} \frac{\partial}{\partial x} \left(Y \frac{\partial \rho}{\partial x} \right) - \frac{1}{105} \rho m_{112} \frac{\partial^2 Y}{\partial x^2} \right] \\ = - \frac{2}{3} \left[\frac{16}{5} \frac{\rho \sqrt{\pi \theta} a^2}{m} Y \right] q_2. \end{aligned} \quad (7.13)$$

Balance equation for kinetic third-order moment m_{112} :

$$\begin{aligned} & \frac{8}{5}\theta \frac{\partial}{\partial x} \left[\left(1 + \frac{6}{35} \frac{2\pi}{3} \frac{a^3}{m} \rho Y \right) \sigma_{12} \right] - \frac{8}{5} \frac{\theta \sigma_{12}}{\rho} \frac{\partial}{\partial x} \left[\rho + \frac{2}{5} \frac{2\pi}{3} \frac{a^3}{m} \rho^2 Y \right] \\ & + \frac{8}{35} \frac{\partial}{\partial x} \left[\left(1 + \frac{12}{35} \frac{2\pi}{3} \frac{a^3}{m} \rho Y \right) R_{12} \right] + \frac{124}{1225} \frac{2\pi}{3} \frac{a^3}{m} \frac{R_{12}}{\rho} \frac{\partial \rho^2 Y}{\partial x} \\ & - \frac{\sqrt{\pi} a^4}{m} \sqrt{\theta} \left[\frac{32}{525} \rho \theta Y \frac{\partial \rho}{\partial x} \frac{\partial v_2}{\partial x} + \frac{16}{525} \rho^2 \theta \frac{\partial}{\partial x} \left(Y \frac{\partial v_2}{\partial x} \right) \right] \\ & - \frac{\sqrt{\pi} a^4}{m} \sqrt{\theta} \left[\frac{72}{875} \rho \frac{\partial}{\partial x} \left(Y \frac{\partial q_2}{\partial x} \right) - \frac{8}{75} q_2 \frac{\partial}{\partial x} \left(Y \frac{\partial \rho}{\partial x} \right) - \frac{16}{2625} \rho q_2 \frac{\partial^2 Y}{\partial x^2} \right] \\ & - \frac{\sqrt{\pi} a^4}{m} \sqrt{\theta} \left[\frac{3}{25} \rho \frac{\partial}{\partial x} \left(Y \frac{\partial m_{112}}{\partial x} \right) - \frac{37}{35} m_{112} \frac{\partial}{\partial x} \left(Y \frac{\partial \rho}{\partial x} \right) - \frac{41}{175} \rho m_{112} \frac{\partial^2 Y}{\partial x^2} \right] \\ & = -\frac{24}{5} \frac{\rho \sqrt{\pi} \theta a^2}{m} Y m_{112}. \end{aligned} \tag{7.14}$$

Balance equation for kinetic fourth-order moment R_{12} :

$$\begin{aligned} & \frac{14}{5}\theta \frac{\partial}{\partial x} \left[\left(1 + \frac{12}{35} \frac{2\pi}{3} \frac{a^3}{m} \rho Y \right) q_2 \right] - \frac{14}{5} \theta \frac{q_2}{\rho} \frac{\partial}{\partial x} \left[\left(1 + \frac{1}{2} \frac{2\pi}{3} \frac{a^3}{m} \rho Y \right) \rho \right] \\ & + 2\theta \frac{\partial}{\partial x} \left[\left(1 + \frac{12}{35} \frac{2\pi}{3} \frac{a^3}{m} \rho Y \right) m_{112} \right] - 2 \frac{m_{112} \theta}{\rho} \frac{\partial}{\partial x} \left[\left(1 + \frac{11}{14} \frac{2\pi}{3} \frac{a^3}{m} \rho Y \right) \rho \right] \\ & - \frac{a^4 \sqrt{\pi}}{m} \sqrt{\theta} \left[\frac{8}{35} \rho \theta \frac{\partial}{\partial x} \left(Y \frac{\partial \sigma_{12}}{\partial x} \right) - \frac{8}{15} \theta \sigma_{12} \frac{\partial}{\partial x} \left(Y \frac{\partial \rho}{\partial x} \right) - \frac{8}{105} \rho \theta \sigma_{12} \frac{\partial^2 Y}{\partial x^2} \right] \\ & - \frac{a^4 \sqrt{\pi}}{m} \sqrt{\theta} \left[\frac{12}{49} \rho \frac{\partial}{\partial x} \left(Y \frac{\partial R_{12}}{\partial x} \right) - \frac{704}{735} R_{12} \frac{\partial}{\partial x} \left(Y \frac{\partial \rho}{\partial x} \right) - \frac{131}{735} \rho R_{12} \frac{\partial^2 Y}{\partial x^2} \right] \\ & = - \left[\frac{16}{5} \frac{a^2 \rho \sqrt{\pi} \theta}{m} Y \right] \left(\frac{1}{2} \theta \sigma_{12} + \frac{205}{168} R_{12} \right). \end{aligned} \tag{7.15}$$

The system of five linear second-order ordinary differential equations (7.11)–(7.15) defines a boundary-value problem, once it is prescribed that at $x = 0$ and far from the interface the Navier–Stokes solution for a uniform shear flow holds.

The linearity allows us to consider approximations of intermediate complexity, with respect to the above full set of five equations. The simplest one, named *2-modes approximation*, consists in forcing $q_2 = m_{112} = R_{12} = 0$ and describing the flow by (7.11) and (7.12). It is interesting to note that the 2-modes approximation provides the correct Navier–Stokes solution in the regions of uniform density but it does not coincide with the isothermal DIM description of the interface flow.

Grad’s 13-moments approximation is obtained by describing the flow by the fields $v_2(x)$, $\sigma_{12}(x)$, $q_2(x)$, governed by (7.11)–(7.13) with $m_{112} = R_{12} = 0$.

The equations associated with the approximations described above have been solved by turning them into linear algebraic systems, through quite standard discretization methods. The coefficients of the unknowns and their derivatives have been computed by approximating the unperturbed density profile by a hyperbolic tangent profile, matched to the solution of (7.3) (Frezzotti *et al.* 2005).

Moment equations solutions have been compared to DSMC (stochastic) solutions of the EV equation, tailored to the considered Couette flow configuration.

In DSMC, two infinite planar and parallel walls are located at positions $x = \pm x_w$, where x is the coordinate spanning the direction normal to the walls. The central part of the gap between the walls is occupied by a liquid slab of width $2x_l$, surrounded by two symmetrically located gas regions of width $x_w - x_l$. A simple steady shear flow is generated in the two-phase fluid by assigning velocities $\pm U_w \hat{y}$ to the walls at $x = \pm x_w$, where \hat{y} is a unit vector parallel to the walls. It is further assumed that gas molecules hitting walls are re-emitted with velocities distributed according to Maxwellians characterized by wall velocities $\pm U_w \hat{y}$ and temperature T_w . A thermostat keeps the central part of the liquid slab at temperature T_w , thus absorbing the energy dissipated into the system by shear stresses.

The results presented below have been obtained by time-averaging the velocities of 24 million particles over about 10^5 time steps, after the onset of a steady solution. The large sample size is necessary to resolve the small deviation from equilibrium required by the comparison of the DSMC solution of the nonlinear EV equation with solutions of the linearized moment equations. In this respect, it is worth mentioning that although the DSMC shear rate, tuned by U_w , has been set as small as permitted by the noise-to-signal ratio, the DSMC solution is not exactly isothermal. In the preliminary example shown below, the normalized equilibrium temperature has been set equal to 0.6. The DSMC shows a slight temperature maximum of 0.605 next to the liquid–vapour interface. Although further numerical work is required, we believe that the present accuracy level is sufficient to judge the quality of the moment formulation described above.

We proceed with comparing results from EV26 and DSMC. Due to the large sample size required, the computational time for DSMC is relatively large, about 24 hours, on a workstation equipped with a 10-core CPU. We note that DSMC requires unsteady three-dimensional simulations (with periodic boundaries in the y, z directions). In contrast, this one-dimensional problem can be solved in about one minute with the moment equations, which benefit from a lower number of variables, the dimensional reduction, steadiness and linearity of the problem formulation.

Figure 4 shows velocity v_2 , kinetic shear stress σ_{12} , kinetic heat flux q_2 , and moments m_{112} , R_{12} for dimensionless temperature $\theta = 0.6 \simeq 0.8 \times \theta_{crit}$, as computed from the 26 moment system, the reduced system with 13 moments (variables $\rho, v_2, \sigma_{12}, q_2$), and the further reduced 2-mode system (variables ρ, v_2, σ_{12}). The results are compared with the DSMC solution of the EV equation itself (Frezzotti 1997) that serves as a reference.

The main features of the flow field can be seen in figure 4(a), where the velocity field exhibits the structure of two uniform shear flows in the liquid and vapour regions, respectively, connected by the interface flow region. The macroscopically sharp change in velocity over the interface is a resolved slip effect, which would be dealt with as a slip boundary condition in a traditional hydrodynamic context. As can be seen from figures 4(a) and 4(b), moment theories with 26 and 13 moments give very good agreement to DSMC for velocity v_2 and kinetic stress σ_{12} . The 2-mode model does not succeed in approximating the velocity change across the interface, predicting a too-weak velocity slip.

The kinetic heat flux q_2 shown in figure 4(c) is due to forced gas motion, and not driven by a temperature gradient. Such a contribution to heat flux does not occur in classical hydrodynamics (Navier–Stokes–Fourier), but is well known in rarefied gas dynamics (Struchtrup 2005). The heat flux computed from the 26 moment system is in reasonably good agreement with the DSMC result, while the 13 moments theory clearly overpredicts

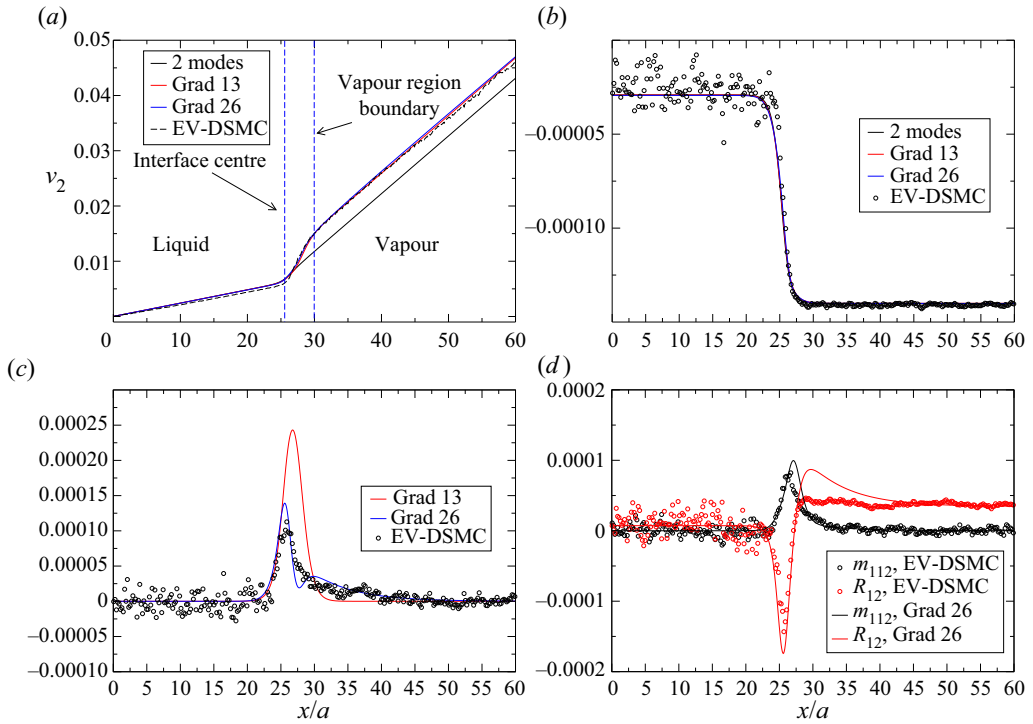


Figure 4. Two-phase Couette flow: comparison of EV DSMC and linearized moment equations, in the case $\theta = 0.6$. (a) Shear velocity v_2 ; (b) kinetic shear stress σ_{12} ; (c) kinetic heat flux component q_2 ; (d) third- and fourth-order moments m_{112} and R_{12} .

the heat flux. This indicates the importance of including higher-order moments (m_{112} , R_{12}), which have clear influence on process detail around the interface. As can be seen in figure 4(d), the 26 moment system gives a good approximation for m_{112} , while somewhat overpredicting the value of R_{12} in the vapour in front of the interface. While velocity and stress variations are confined to the interfacial region as defined through the density variation, the higher moments (q_2 , m_{112} , R_{12}) exhibit variations further into the vapour – these are Knudsen layer contributions.

8. Conclusions

In this contribution we have presented the derivation of a set of 26 moment equations from the Enskog–Vlasov equation, (6.1)–(6.13). The moment equations describe liquids and vapours, either alone or in contact through one or several continuous phase interfaces. If considered for single phases, then the equations describe either a somewhat compressible liquid, or a non-ideal gas of van-der-Waals-type. In the limit of small densities, the equations reduce to the (linearized) 26 moment equations for rarefied ideal gases.

Just as with higher-order moment equations for ideal gases, the equations describe higher-order transport effects, such as thermal stresses, non-Fourier heat flux and Knudsen layers. While 13 moment equations for Enskog gases were presented before (Kremer & Rosa 1988), this appears to be the first time that a moment system for the EV equation was developed. We note that for ideal gases, 13 moments do not suffice to describe Knudsen layer effects, which, however, can be approximated with 26 moments.

We emphasize that in this first approach to a set of macroscopic equations with resolved phase interface and Knudsen layers, we relied on linearizations as well as Taylor expansions with the particle size. Specifically, we ignored all nonlinear terms involving non-equilibrium properties, so that only nonlinear terms with the density gradient – which is significant in the interface – remain in the equations.

The resolved interface has a thickness of the order of 10 atomic diameters a , with larger values closer to the critical point. Hence tracking of property changes across the interface requires high resolution. As of now, our expansions in particle size account for non-equilibrium terms up to fourth order, while fifth-order contributions are included only for the equilibrium terms in the capillary stresses. Our results so far indicate that agreement with DSMC solutions of the EV equations is good not too far from the critical point, where the interface is wider, and differences between liquid and vapour equilibrium states are smaller (recall that all differences vanish at the critical point).

Further from the critical point, where the interface is thinner, and differences between vapour and liquid are stronger, we observe more marked deviations. It might well be that to capture these states, higher-order terms – fifth- or higher-order in a – should be included in the equations. This option will be considered in the future, based on a careful analysis of the equations, and the expansion procedure. Deriving and several rounds of double-checking of the (mainly) fourth-order equations led us to develop better strategies that in the future will allow us to add higher-order terms in a more efficient manner compared to our first steps towards the equations presented above.

The EV26 moment equations open an array of avenues for future work. Further comparison with DSMC solutions is required to understand their appropriate range of applicability as well as which additional higher-order terms (from expansion, or nonlinear terms) should be added to increase their range.

DSMC and molecular dynamics solutions are expensive computationally and affected by stochastic noise, in particular for flows exhibiting small deviations from equilibrium. In contrast to this, the EV26 moment equations require far fewer resources for their deterministic noise-free solutions. With that, they offer the opportunity to study a wide variety of single-phase and two-phase flows with evaporation/condensation, such as Couette flow, heat transfer and forced evaporation, all for a wide range of parameters.

Our preliminary results show the expected steep gradients in the interface, which lead to effective velocity slip phenomena across the interface. Detailed accounts of solutions, the discussion of interface phenomena, and the determination of jump, slip and evaporation coefficients in dependence of state of the interface and process parameters, are planned for the future. Another line of work will consider the equations in the bulk phases – liquid and vapour – with questions concerning model reduction (Struchtrup & Torrilhon 2013), wave speed and damping, and the development of wall boundary conditions.

Funding. H.S. gratefully acknowledges support from the National Sciences and Engineering Research Council (NSERC), grant no. RGPIN-2016-03679.

Declaration of interests. The authors report no conflict of interest.

Author ORCIDs.

 Henning Struchtrup <https://orcid.org/0000-0002-4986-0728>;

 Aldo Frezzotti <https://orcid.org/0000-0003-3858-1536>.

Appendix A. *k*-integrals

The integrals $[I_{m,n}^\alpha]_{i_1 \dots i_{n+m}}$ of (5.23) must be symmetric linear combinations of the unit tensor δ_{ij} and $g_i = \{0, 0, g\}$, and here we show those integrals that were required in the process of finding our final transport equations for 26 variables. For $n = m = 0$:

$$I_{0,0}^\alpha = \frac{2\pi}{\alpha + 1} g^\alpha. \tag{A1}$$

For $n + m = 1$ (with $m = 0, 1$):

$$[I_{m,1-m}^\alpha]_i = g^{2+\alpha-m} \int_0^{2\pi} \int_0^{\pi/2} k_i \cos^{2+\alpha-m} \theta \sin \theta \, d\theta \, d\varepsilon = \frac{2\pi}{4 + \alpha - m} \frac{g_i}{g^{m-1-\alpha}}. \tag{A2}$$

For $n + m = 2$ (with $m = 0, 1, 2$):

$$[I_{m,2-m}^\alpha]_{ij} = \frac{2\pi}{(6 + \alpha - m)(4 + \alpha - m)} \left(\frac{\delta_{ij}}{g^{m-3-\alpha}} + (3 + \alpha - m) \frac{g_i g_j}{g^{m-1-\alpha}} \right). \tag{A3}$$

For $n + m = 3$ (with $m = 0, 1, 2, 3$):

$$[I_{m,3-m}^\alpha]_{ijk} = \frac{2\pi}{(8 + \alpha - m)(6 + \alpha - m)} \left(3 \frac{\delta_{(ij} \delta_{k)}}{g^{m-3-\alpha}} + (3 + \alpha - m) \frac{g_i g_j g_k}{g^{m-1-\alpha}} \right). \tag{A4}$$

For $n + m = 4$ (with $m = 1, 2, 3$):

$$[I_{m,4-m}^0]_{ijkl} = \frac{2\pi}{(10 - m)(8 - m)(6 - m)} \left(3 \frac{\delta_{(ij} \delta_{kl)}}{g^{m-5}} + 6(5 - m) \frac{\delta_{(ij} \delta_{k} g_l)}{g^{m-3}} + (15 - 8m + m^2) \frac{g_i g_j g_k g_l}{g^{m-1}} \right). \tag{A5}$$

For $n + m = 5$ (with $m = 2, 3$):

$$[I_{m,5-m}^\alpha]_{ijklr} = \frac{2\pi}{(12 + \alpha - m)(10 + \alpha - m)(8 + \alpha - m)} \times \left(15 \frac{\delta_{(ij} \delta_{kl} g_r)}{g^{m-5-\alpha}} + 10(5 + \alpha - m) \frac{\delta_{(ij} \delta_{k} g_l g_r)}{g^{m-3-\alpha}} + (5 + \alpha - m)(3 + \alpha - m) \frac{g_i g_j g_k g_l g_r}{g^{m-1-\alpha}} \right). \tag{A6}$$

For $n + m = 6$ (we needed only one integral):

$$[I_{3,3}^0]_{ijkrst} = \frac{2\pi}{231} g^4 \delta_{(ij} \delta_{kr} \delta_{st)} + \frac{8\pi}{77} g^2 \delta_{(ij} \delta_{kr} g_s g_t) + \frac{16\pi}{231} \delta_{(ij} g_k g_r g_s g_t). \tag{A7}$$

Appendix B. Integrals for momentum balance

B.1. *Integrals over $f^1 f$*

With the 26 moment distribution, $f|_{26} = \hat{f}_M(\rho + \Phi)$, the product $f^1 f$ is of the form, after linearization in non-equilibrium quantities,

$$f^1 f = \hat{f}_M^1 \hat{f}_M (\rho^2 + \rho (\Phi + \Phi^1)). \tag{B1}$$

The resulting integrals are tensors that are linear combinations of the unit tensor and the tensorial moments, with coefficients that depend on density and temperature.

We show only integrals required for the momentum balance:

$$\int \int f^1 f \{g_i g_i\} d\mathbf{c}^1 d\mathbf{c} = 0, \quad (\text{B2})$$

$$\int \int f^1 f \{g_i g_r\} d\mathbf{c}^1 d\mathbf{c} = 2 \frac{\rho^2 \theta}{m^2} \delta_{ir} + 2 \frac{\rho}{m^2} \sigma_{ir}. \quad (\text{B3})$$

The trace of this gives

$$\int \int f^1 f \left\{ g^2 \delta_{ir} \right\} d\mathbf{c}^1 d\mathbf{c} = 6 \frac{\rho^2 \theta}{m^2} \delta_{ir}. \quad (\text{B4})$$

This 3-tensor vanishes:

$$\int \int f^1 f \left\{ \frac{g_i g_r g_s}{g} \right\} d\mathbf{c}^1 d\mathbf{c} = 0. \quad (\text{B5})$$

B.2. Integrals over $\partial^n f_1 / \partial x^n f$

The derivative of f_{j26} is given in (5.10). In compact notation, we write

$$\frac{\partial^n f_1}{\partial} = \hat{f}_M^1 D\Psi^1, \quad (\text{B6})$$

where $D\Psi$ is a polynomial in C_i with factors that depend on the derivatives of all variables that can be identified from (5.10). The semi-linearized product is

$$\frac{\partial^n f_1}{\partial} f = \hat{f}_M^1 f_M (\rho + \Phi) D\Phi^1 = \hat{f}_M^1 f_M \left(\rho D\Psi^1 + \Phi D\rho \right). \quad (\text{B7})$$

In the results, we keep nonlinear terms of non-equilibrium quantities with density gradient, but linear terms otherwise. Again, we show only integrals required for the momentum balance.

In the compact notation, introduced above, we find

$$\int \int \frac{\partial^n f_1}{\partial} f \{g_i g_s\} d\mathbf{c}^1 d\mathbf{c} = \frac{16}{3} \frac{\rho \theta}{m^2 \sqrt{\pi \theta}} \mathcal{A}_{[\cdot], s} + \frac{8}{15} \frac{\rho}{m^2 \sqrt{\pi \theta}} \frac{\partial^n q_s}{\partial} - \frac{8}{15} \frac{\rho}{m^2 \sqrt{\pi \theta}} \frac{q_s}{\rho} \frac{\partial^n \rho}{\partial}. \quad (\text{B8})$$

To clarify the compact notation, we show the case of the second derivative, where

$$\begin{aligned} \int \int \frac{\partial^2 f_1}{\partial x_i \partial x_j} f \{g_i g_s\} d\mathbf{c}^1 d\mathbf{c} &= \frac{16}{3} \frac{\rho \theta}{m^2 \sqrt{\pi \theta}} \mathcal{A}_{[ij], s} + \frac{8}{15} \frac{\rho}{m^2 \sqrt{\pi \theta}} \frac{\partial^2 q_s}{\partial x_i \partial x_j} \\ &\quad - \frac{8}{15} \frac{\rho}{m^2 \sqrt{\pi \theta}} \frac{q_s}{\rho} \frac{\partial^2 \rho}{\partial x_i \partial x_j}. \end{aligned} \quad (\text{B9})$$

Other integrals used, shown in compact notation only, are

$$\int \int \frac{\partial^n f_1}{\partial} f \{g_i g_r\} d\mathbf{c}^1 d\mathbf{c} = \frac{\rho}{m^2} \left(2\theta \frac{\partial \rho}{\partial} + \mathcal{B}_{[\cdot]} \right) \delta_{ir} + \frac{\rho}{m^2} \left(\frac{\partial \sigma_{ir}}{\partial} + \frac{\sigma_{ir}}{\rho} \frac{\partial \rho}{\partial} \right), \quad (\text{B10})$$

with trace

$$\int \int \frac{\partial^n f^1}{\partial} \{g^2\} d\mathbf{c}^1 d\mathbf{c} = 3 \frac{\rho}{m^2} \left(2\theta \frac{\partial \rho}{\partial} + \mathcal{B}_{[1]} \right), \tag{B11}$$

and

$$\begin{aligned} \int \int \frac{\partial f^1}{\partial} f \left\{ \frac{g_i g_r g_s}{g} \right\} d\mathbf{c}^1 d\mathbf{c} &= \frac{16}{5} \frac{\rho}{m^2 \sqrt{\pi \theta}} \theta \delta_{(ir} \mathcal{A}_{[1],s)} \\ &+ \frac{8}{25} \frac{\rho}{m^2 \sqrt{\pi \theta}} \left(\delta_{(ir} \frac{\partial q_s}{\partial} - \frac{\delta_{(ir} q_s}{\rho} \frac{\partial \rho}{\partial} \right) + \frac{16}{35} \frac{\rho}{m^2 \sqrt{\pi \theta}} \left(\frac{\partial m_{irs}}{\partial} - \frac{m_{irs}}{\rho} \frac{\partial \rho}{\partial} \right). \end{aligned} \tag{B12}$$

Appendix C. Correction for equal area rule

For the one-dimensional case, Aifantis & Serrin (1983) write the capillary pressure terms in general notation as

$$P_{cap} = \alpha \frac{\partial^2 \rho}{\partial x^2} + \beta \frac{\partial \rho}{\partial x} \frac{\partial \rho}{\partial x}, \tag{C1}$$

where α and β depend on local density. They find that for validity of the equal area rule, these coefficients must be related as

$$\beta = \frac{1}{2} \rho^2 \frac{d}{d\rho} \left(\frac{\alpha}{\rho^2} \right) = \frac{1}{2} \frac{d\alpha}{d\rho} - \frac{\alpha}{\rho}. \tag{C2}$$

The relationship between α and β is linear, so that common factors can be taken out of the discussion, as below.

In the EV momentum balance (6.2), we find (in one dimension) the normal capillary stress from the Vlasov contribution as

$$P_{Vlasov} = -\frac{2\pi}{15} \frac{a^5}{m} \phi_a \chi_3 \left[\rho \frac{\partial^2 \rho}{\partial x^2} - \frac{1}{2} \frac{\partial \rho}{\partial x} \frac{\partial \rho}{\partial x} \right], \tag{C3}$$

from which we identify $\alpha = \rho$, $\beta = -\frac{1}{2}$, which fulfil the condition (C2):

$$\frac{1}{2} \frac{d\alpha}{d\rho} - \frac{\alpha}{\rho} = \frac{1}{2} - 1 = -\frac{1}{2} = \beta. \tag{C4}$$

The Enskog contribution mixes density and temperature effects as, in one dimension,

$$P_{Enskog} = \frac{\pi}{60} \frac{a^5}{m} \left[\frac{\partial^2 Y \rho^2 \theta}{\partial x^2} + 3Y \frac{\partial^2 \rho^2 \theta}{\partial x^2} - 12Y \frac{\partial \rho}{\partial x} \frac{\partial \rho \theta}{\partial x} \right]. \tag{C5}$$

In equilibrium, temperature is a constant, and the above reduces (with $Y' = dY/d\rho$, etc.) to

$$P_{Enskog} = \frac{\pi}{60} \frac{a^5}{m} \theta \left[(8\rho Y + \rho^2 Y') \frac{\partial^2 \rho}{\partial x^2} + (4Y' \rho + \rho^2 Y'' - 4Y) \frac{\partial \rho}{\partial x} \frac{\partial \rho}{\partial x} \right], \tag{C6}$$

and we identify

$$\alpha = 8\rho Y + \rho^2 Y', \quad \beta = 4Y' \rho + \rho^2 Y'' - 4Y. \tag{C7a,b}$$

We evaluate

$$\frac{1}{2} \frac{d\alpha}{d\rho} - \frac{\alpha}{\rho} = 4\rho Y' + \frac{1}{2} \rho^2 Y'' - 4Y = \beta - \frac{1}{2} \rho^2 Y'' = \hat{\beta}. \quad (\text{C8})$$

That is, there is a mismatch ($-\frac{1}{2}\rho^2 Y''$) with respect to the condition (C2), hence the Enskog contribution violates the equal area rule.

To reinstate the equal area rule, we can simply replace β by $\hat{\beta}$ as introduced above, so that for the isothermal case (Barbante 2016),

$$P_{\text{Enskog}} = \frac{\pi}{60} \frac{a^5}{m} \theta \left[\frac{\partial^2 Y \rho^2}{\partial x^2} + 3Y \frac{\partial^2 \rho^2}{\partial x^2} - 12Y \frac{\partial \rho}{\partial x} \frac{\partial \rho}{\partial x} - \frac{1}{2} \rho^2 Y'' \frac{\partial \rho}{\partial x} \frac{\partial \rho}{\partial x} \right]. \quad (\text{C9})$$

For the non-isothermal case, we just use the same term, i.e.

$$P_{\text{Enskog}} = \frac{\pi}{60} \frac{a^5}{m} \left[\frac{\partial^2 Y \rho^2 \theta}{\partial x^2} + 3Y \frac{\partial^2 \rho^2 \theta}{\partial x^2} - 12Y \frac{\partial \rho}{\partial x} \frac{\partial \rho \theta}{\partial x} - \frac{1}{2} \theta \rho^2 Y'' \frac{\partial \rho}{\partial x} \frac{\partial \rho}{\partial x} \right]. \quad (\text{C10})$$

All original terms have temperature under space derivatives. Considering the *ad hoc* nature of the correction, we best use the above, which does not alter the thermal response to non-equilibrium. The extension to three dimensions in (7.8) is based on the form of the original Enskog contributions.

REFERENCES

- AIFANTIS, E.C. & SERRIN, J.B. 1983 The mechanical theory of fluid interfaces and Maxwell's rule. *J. Colloid Interface Sci.* **96**, 517–529.
- ANDERSON, D.M., MCFADDEN, G.B. & WHEELER, A.A. 1998 Diffusive-interface methods in fluid mechanics. *Annu. Rev. Fluid Mech.* **30**, 139–165.
- BALESCU, R. 1975 *Equilibrium and Nonequilibrium Statistical Mechanics*. John Wiley & Sons.
- BARBANTE, B. 2016 private communication. Politecnico di Milano.
- BARBANTE, P. & FREZZOTTI, A. 2017 A comparison of models for the evaporation of the Lennard-Jones fluid. *Eur. J. Mech. B/Fluids* **64**, 69–80.
- BECKMANN, A.F., RANA, A.S., TORRILHON, M. & STRUCHTRUP, H. 2018 Evaporation boundary conditions for the linear R13 equations based on the Onsager theory. *Entropy* **20**, 680.
- BENILOV, E.S. & BENILOV, M.S. 2018 Energy conservation and H theorem for the Enskog–Vlasov equation. *Phys. Rev. E* **97** (6), 062115.
- BIRD, G.A. 1994 *Molecular gas dynamics and the direct simulation of gas flows*. Oxford University Press.
- BOBYLEV, A.V. 1982 The Chapman–Enskog and Grad methods for solving the Boltzmann equation. *Sov. Phys. Dokl.* **27**, 29–31.
- BOND, M. & STRUCHTRUP, H. 2004 Mean evaporation and condensation coefficients based on energy dependent condensation probability. *Phys. Rev. E* **70**, 061605.
- BRUNO, D. & FREZZOTTI, A. 2019 Dense gas effects in the Rayleigh–Brillouin scattering spectra of SF_6 . *Chem. Phys. Lett.* **731**, 136595.
- BURNETT, D. 1936 The distribution of molecular velocities and the mean motion in a non-uniform gas. *Proc. Lond. Math. Soc.* **40**, 382–435.
- BUSUIOC, S. & GIBELLI, L. 2020 Mean-field kinetic theory approach to Langmuir evaporation of polyatomic liquids. *Phys. Fluids* **32**, 093314.
- CAPUTA, J.P. & STRUCHTRUP, H. 2011 Interface model for non-equilibrium evaporation. *Physica A* **390**, 31–42.
- CARNAHAN, N.F. & STARLING, K.E. 1969 Equation of state for nonattracting rigid spheres. *J. Chem. Phys.* **51**, 635–636.
- CERCIGNANI, C. 1975 *Theory and Application of the Boltzmann Equation*. Scottish Academic Press.
- CHAPMAN, S. & COWLING, T.G. 1970 *The Mathematical Theory of Non-Uniform Gases*. Cambridge University Press.
- CIPOLLA, J.W., LANG, H. & LOYALKA, S.K. 1974 Kinetic theory of condensation and evaporation. II. *J. Chem. Phys.* **61**, 69–78.

- EAMES, I., MARR, N. & SABIR, H. 1997 The evaporation coefficient of water: a review. *Intl J. Heat Mass Transfer* **40**, 2963–2973.
- ENSKOG, D. 1921 The numerical calculation of phenomena in fairly dense gases. *Ark. Mat. Astron. Fys.* **16** (1), 1–60.
- FREZZOTTI, A. 1997 A particle scheme for the numerical solution of the Enskog equation. *Phys. Fluids* **9**, 1329–1335.
- FREZZOTTI, A. 1998 Molecular dynamics and Enskog theory calculation of shock profiles in a dense hard sphere gas. *Comput. Maths Applics.* **35** (1–2), 103–112.
- FREZZOTTI, A. 1999 Monte Carlo simulation of the heat flow in a dense hard sphere gas. *Eur. J. Mech. B/Fluids* **18** (1), 103–119.
- FREZZOTTI, A. 2011 Boundary conditions at the vapor-liquid interface. *Phys. Fluids* **23** (3), 030609.
- FREZZOTTI, A. & BARBANTE, P. 2020 Simulation of shock induced vapor condensation flows in the Lennard-Jones fluid by microscopic and continuum models. *Phys. Fluids* **32** (12), 122106.
- FREZZOTTI, A., BARBANTE, P. & GIBELLI, L. 2019 Direct simulation Monte Carlo applications to liquid-vapor flows. *Phys. Fluids* **31** (6), 062103.
- FREZZOTTI, A., GIBELLI, L., LOCKERBY, D. & SPRITTLES, J.E. 2018 Mean-field kinetic theory approach to evaporation of a binary liquid into vacuum. *Phys. Rev. Fluids* **3** (5), 054001.
- FREZZOTTI, A., GIBELLI, L. & LORENZANI, S. 2005 Mean field kinetic theory description of evaporation of a fluid into vacuum. *Phys. Fluids* **17**, 012102.
- FREZZOTTI, A., GROSFILS, P. & TOXVAERD, S. 2003 Evidence of an inverted temperature gradient during evaporation/condensation of a Lennard-Jones fluid. *Phys. Fluids* **15**, 2837–2842.
- FREZZOTTI, A. & ROSSI, M. 2012 Slip effects at the vapor-liquid boundary. *AIP Conf. Proc.* **1501**, 903–910.
- FREZZOTTI, A. & STEFANOV, S. 1995 DSMC analysis of the evaporation of iodine between parallel plates. In *Proc. of 19th. Int. RGD Symp.* (ed. J. Harvey & G. Lord), vol. 1, pp. 298–304. Oxford Science Publications.
- GIOVANGIGLI, V. 2020 Kinetic derivation of diffuse-interface fluid models. *Phys. Rev. E* **102**, 012110.
- GRAD, H. 1949 On the kinetic theory of rarefied gases. *Commun. Pure Appl. Maths* **2**, 331–407.
- GRAD, H. 1958 Principles of the kinetic theory of gases. In *Handbuch der Physik XII: Thermodynamik der Gase* (ed. S. Flügge). Springer.
- GRMELA, M. 1971 Kinetic equation approach to phase transitions. *J. Stat. Phys.* **3**, 347–364.
- GUPTA, V. & TORRILHON, M. 2012 Automated Boltzmann collision integrals for moment equations. In *Proc. 28th Symp. on Rarefied Gas Dynamics, Zaragoza, Spain 2012* (ed. M. Mareschal *et al.*), AIP Conf. Proc., vol. 1501, pp. 67–74. AIP Publishing.
- HERTZ, H. 1882 Über die Verdunstung der Flüssigkeiten, insbesondere des Quecksilbers, im luftleeren Raume. *Ann. Phys.* **253**, 177–193.
- JONES, J.E. 1924 On the determination of molecular fields. I. From the variation of the viscosity of a gas with temperature. *Proc. Math. Phys. Engng Sci.* **106** (738), 441–462.
- KARKHECK, J. & STELL, G. 1981 Mean field kinetic theories. *J. Chem. Phys.* **75**, 1475–1487.
- KJELSTRUP, S. & BEDEAUX, D. 2008 *Non-Equilibrium Thermodynamics of Heterogeneous Systems*. World Scientific.
- KNUDSEN, M. 1915 Die maximale Verdampfungsgeschwindigkeit des Quecksilbers. *Ann. Phys.* **352**, 697–708.
- KON, M., KOBAYASHI, K. & WATANABE, M. 2014 Method of determining kinetic boundary conditions in net evaporation/condensation. *Phys. Fluids* **26** (7), 072003.
- KREMER, G.M. 2010 *An Introduction to the Boltzmann Equation and Transport Processes in Gases*. Springer.
- KREMER, G.M. & ROSA, E. JR. 1988 On Enskog's dense gas theory. I. The method of moments for monatomic gases. *J. Chem. Phys.* **89**, 3240–3247.
- MAGER, R., ADOMEIT, G. & WORTBERG, G. 1989 Theoretical and experimental investigation of the strong evaporation of solids. In *Rarefied Gas Dynamics* (ed. P. Muntz), vol. 117, pp. 460–469. AIAA.
- MAREK, R. & STRAUB, J. 2001 Analysis of the evaporation coefficient and the condensation coefficient of water. *Intl J. Heat Mass Transfer* **44**, 39–53.
- PAO, Y.P. 1971a Application of kinetic theory to the problem of evaporation and condensation. *Phys. Fluids* **14**, 306–312.
- PAO, Y.P. 1971b Temperature and density jumps in the kinetic theory of gases and vapors. *Phys. Fluids* **14**, 1340–1346.
- PIECHÓR, K. 2008 Non-local Korteweg stresses from kinetic theory point of view. *Arch. Mech.* **60** (1), 23–58.
- RAH, K. & EU, B.C. 2001 Theory of non-equilibrium liquid-vapor interface: effects of shear. *Physica A* **292**, 102–128.
- RESIBOIS, P. 1978 H-theorem for the modified nonlinear Enskog equation. *J. Stat. Phys.* **19** (6), 593–609.
- RESIBOIS, P. & DE LEENER, M. 1977 *Classical Kinetic Theory of Fluids*. Wiley.
- SCHRAGE, R.W. 1953 *A Theoretical Study of Interphase Mass Transfer*. Columbia University Press.

Twenty-six moment equations for the Enskog–Vlasov equation

- SHAVALIYEV, M.S. 1993 Super-Burnett corrections to the stress tensor and the heat flux in a gas of Maxwellian molecules. *Z. Angew. Math. Mech.* **57** (3), 573–576.
- DE SOBRINO, L. 1967 On the kinetic theory of a van der Waals gas. *Can. J. Phys.* **45**, 363–385.
- SONE, Y. 2000 Kinetic theoretical studies of the half-space problem of evaporation and condensation. *Transp. Theory Stat. Phys.* **29**, 227–260.
- STRUCHTRUP, H. 2004 Stable transport equations for rarefied gases at high orders in the Knudsen number. *Phys. Fluids* **16** (11), 3921–3934.
- STRUCHTRUP, H. 2005 *Macroscopic Transport Equations for Rarefied Gas Flows – Approximation Methods in Kinetic Theory*, Interaction of Mechanics and Mathematics Series. Springer.
- STRUCHTRUP, H. 2014 *Thermodynamics and Energy Conversion*. Springer.
- STRUCHTRUP, H., BECKMANN, A.F., RANA, A.S. & FREZZOTTI, A. 2017 Evaporation boundary conditions for the R13 equations of rarefied gas dynamics. *Phys. Fluids* **29**, 092004.
- STRUCHTRUP, H. & TORRILHON, M. 2003 Regularization of Grad’s 13 moment equations: derivation and linear analysis. *Phys. Fluids* **15** (9), 2668–2680.
- STRUCHTRUP, H. & TORRILHON, M. 2007 H-theorem, regularization, and boundary conditions for linearized 13 moment equations. *Phys. Rev. Lett.* **99**, 014502.
- STRUCHTRUP, H. & TORRILHON, M. 2013 Regularized 13 moment equations for hard sphere molecules: linear bulk equations. *Phys. Fluids* **25**, 052001.
- SUTHERLAND, W. 1893 The viscosity of gases and molecular force. *Lond. Edinb. Dublin Philos. Mag. J. Sci.* **36** (293), 507–531.
- TORRILHON, M. 2016 Modeling nonequilibrium gas flow based on moment equations. *Annu. Rev. Fluid Mech.* **48**, 429–458.
- TORRILHON, M. & STRUCHTRUP, H. 2008 Boundary conditions for regularized 13-moment-equations for micro-channel-flows. *J. Comput. Phys.* **227**, 1982–2011.
- VAN BEIJEREN, H. & ERNST, M.H. 1973 The modified Enskog equation. *Physica A* **68**, 437–456.
- VLASOV, A.A. 1961 *Many-Particle Theory and its Application to Plasma*. Gordon and Breach.
- YTREHUS, T. 1975 Kinetic theory description and experimental results for vapor motion in arbitrary strong evaporation. *Tech. Note* 112. von Kármán Institute for Fluid Dynamics.